Analyzing Stellar Velocity Dispersion During Galaxy Mergers

Nathaniel R. Stickley

Department of Physics & Astronomy

UNIVERSITY OF CALIFORNIA
UCRIVERSIDE

Outline

Section Overview

In order to understand my research, you need to know what stellar velocity dispersion is. . .

- Basic definitions.
- Performing measurements.

Basic Definitions

In **collisionless** systems:

- Particles behave as though they are interacting with a smooth potential.
- Individual particle-particle interactions are less important than interaction with global potential.

Basic Definitions

In **collisionless** systems:

- Particles behave as though they are interacting with a smooth potential.
- Individual particle-particle interactions are less important than interaction with global potential.

Dissipationless: Mechanical energy is conserved – not converted into internal thermal energy.

- Stars and dark matter particles are assumed dissipationless in simulations.
- Gas is assumed to be dissipational.

Basic Definitions

Let R and M be the characteristic radius and total mass of a stellar system, respectively, then

$$\rho = 3M/4\pi R^3,$$

Dynamical timescale: Characteristic timescale required for a typical star to move a distance R,

$$t_{dyn} \sim \frac{1}{\sqrt{G\rho}}$$

Basic Definitions

Let R and M be the characteristic radius and total mass of a stellar system, respectively, then

$$\rho = 3M/4\pi R^3,$$

Dynamical timescale: Characteristic timescale required for a typical star to move a distance R,

$$t_{dyn} \sim \frac{1}{\sqrt{G\rho}}$$

- timescale required for virialization $(2T = -V)$.
- shorter in high-density, central regions of the system.

Basic Definitions

Relaxation timescale:

$$t_{relax} \approx \frac{N}{8 \ln N} t_{dyn} \sim \frac{N}{8 \ln N \sqrt{G\rho}}$$

- timescale during which the system cannot be considered collisionless.
- stars lose all "memory" of their initial orbits (due to close encounters).
- timescale required for equipartition of energy

Basic Definitions

Relaxation timescale:

$$t_{relax} \approx \frac{N}{8 \ln N} t_{dyn} \sim \frac{N}{8 \ln N \sqrt{G\rho}}$$

- timescale during which the system cannot be considered collisionless.
- stars lose all "memory" of their initial orbits (due to close encounters).
- timescale required for equipartition of energy
- $t_{relax} \gg H_0^{-1}$ for galaxies (but not GCs), thus stars in galaxies are approximately collisionless...

The Meaning of σ_{ij}^2

For completely collisionless, dissipationless systems, the evolution is described by the **Jeans Equation** (see Appendix V for derivation),

$$\nu \frac{\partial \bar{v}_j}{\partial t} + \nu \bar{v}_i \frac{\partial \bar{v}_j}{\partial x_i} = -\nu \frac{\partial \Phi}{\partial x_j} - \frac{\partial (\nu \sigma_{ij}^2)}{\partial x_i}$$

Where ν is the number density of particles (i.e., stars),
$\bar{v}_i = \bar{v}_i(\mathbf{x}, t)$ is the average velocity of stars in the i direction, and

$$\sigma_{ij}^2 \equiv \overline{(v_i - \bar{v}_i)(v_j - \bar{v}_j)}$$

σ_{ij}^2 is the covariance of (v_i, v_j), AKA the velocity dispersion tensor.

The Meaning of σ_{ij}^2

The Jeans equation is an analog of Euler's momentum conservation equation for inviscid fluid flow.

Jeans:

$$\nu \frac{\partial \bar{v}_j}{\partial t} + \nu \bar{v}_i \frac{\partial \bar{v}_j}{\partial x_i} = -\nu \frac{\partial \Phi}{\partial x_j} - \frac{\partial (\nu \sigma_{ij}^2)}{\partial x_i}$$

Euler:

$$\rho \frac{\partial \mathbf{v}}{\partial t} + \rho(\mathbf{v} \cdot \nabla)\mathbf{v} = -\rho \nabla \Phi - \nabla P$$

The Meaning of σ_{ij}^2

The Jeans equation is an analog of Euler's momentum conservation equation for inviscid fluid flow.

Jeans:

$$\nu\frac{\partial\bar{v}_j}{\partial t}+\nu\bar{v}_i\frac{\partial\bar{v}_j}{\partial x_i}=-\nu\frac{\partial\Phi}{\partial x_j}-\frac{\partial(\nu\sigma_{ij}^2)}{\partial x_i}$$

Euler:

$$\rho\frac{\partial\mathbf{v}}{\partial t}+\rho(\mathbf{v}\cdot\nabla)\mathbf{v}=-\rho\nabla\Phi-\nabla P$$

Thus $\nu\sigma_{ij}^2$ is analogous with pressure; it is a stress tensor.

A Few Comments

- The Jeans equations are useful for making analytic and semi-analytic models of galaxies.
- They are helpful when trying to *understand* galaxies qualitatively.
- Projections of σ_{ij}^2 are observable (see next few slides). This allows comparison between analytic models and observations.

A Few Comments

- The Jeans equations are useful for making analytic and semi-analytic models of galaxies.
- They are helpful when trying to *understand* galaxies qualitatively.
- Projections of σ_{ij}^2 are observable (see next few slides). This allows comparison between analytic models and observations.

However, the derivation assumed...

- The system is completely collisionless
- The system is completely dissipationless
- The number of stars is conserved

Detailed simulations are needed to understand real galaxies.

The meaning of σ_*

The projection of σ_{ij}^2 along the $\hat{n}_i$ direction is

$$\sigma_*^2 = \hat{n}_j \sigma_{ij}^2 \hat{n}_i$$

σ_* is known as the line-of-sight stellar velocity dispersion,

$$\sigma_* = \sqrt{\hat{n}_j \sigma_{ij}^2 \hat{n}_i} = \sqrt{\langle v_n^2 \rangle - \langle v_n \rangle^2}$$

where v_n is the line-of-sight component of the stellar velocity.

The quantity σ_* is observable. . .

Measuring σ_* Observationally

Assumptions:

- The spectrum of the galaxy is the sum of the Doppler-shifted spectra of the constituent stars.
- The flux received is proportional to the number of stars emitting light.

Measuring σ_* Observationally

Assumptions:

- The spectrum of the galaxy is the sum of the Doppler-shifted spectra of the constituent stars.
- The flux received is proportional to the number of stars emitting light.

Basic Steps:

1. Collect a spectrum.
2. Transform spectrum to rest frame (z=0) to obtain F_λ.
3. Select stellar absorption lines to study (e.g., Ca triplet MgIb).
4. Select high S/N template absorption lines for a template star (or stars).

Measuring σ_* Observationally

From here, the details of the various methods differ. All methods are functionally equivalent to...

Measuring σ_* Observationally

From here, the details of the various methods differ. All methods are functionally equivalent to...

5. Construct a model spectrum f_λ from the linear combination of shifted templates T_{λ,v_i},

$$f_\lambda = C_\lambda + \sum_i w_i T_{\lambda,v_i}$$

where C_λ is the continuum flux and w_i are weights.

Measuring σ_* Observationally

From here, the details of the various methods differ. All methods are functionally equivalent to...

5. Construct a model spectrum f_λ from the linear combination of shifted templates T_{λ,v_i},

$$f_\lambda = C_\lambda + \sum_i w_i T_{\lambda,v_i}$$

where C_λ is the continuum flux and w_i are weights.

6. Find the set of w_i which minimize the residual

$$\|F_\lambda - f_\lambda\|^2$$

Measuring σ_* Observationally

By assumption, w_i is proportional to the number of stars with velocity v_i. Thus w_i yields the line of sight velocity distribution (LOSVD).

Measuring σ_* Observationally

By assumption, w_i is proportional to the number of stars with velocity v_i. Thus w_i yields the line of sight velocity distribution (LOSVD).

7. From the LOSVD, compute σ_*.

Note that this is a **flux-weighted** measurement of σ_*.

Measuring σ_* Observationally

By assumption, w_i is proportional to the number of stars with velocity v_i. Thus w_i yields the line of sight velocity distribution (LOSVD).

7. From the LOSVD, compute σ_*.

Note that this is a **flux-weighted** measurement of σ_*.

Galaxy modelers tend to measure σ_* from the actual velocities of particles in the simulation,

$$\sigma_* = \sqrt{\langle v_n^2 \rangle - \langle v_n \rangle^2}$$

Sometimes the mass-weighted means are calculated.

Outline

The $M_{BH} - \sigma_*$ relation

- Through the 1990s and early 2000s,
  - It became evident that essentially *all* galaxies and at least *some* GCs contain nuclear SMBHs.
  - The radio source Sag A^* near the center of the MW was found to be associated with a $\sim 10^6 M_\odot$ SMBH.

The $M_{BH} - \sigma_*$ relation

- Through the 1990s and early 2000s,
  - It became evident that essentially *all* galaxies and at least *some* GCs contain nuclear SMBHs.
  - The radio source Sag A^* near the center of the MW was found to be associated with a $\sim 10^6 M_\odot$ SMBH.
  - Ferrarese & Merritt and Gebhardt et al. discovered a (relatively) tight relationship between M_{BH} and central σ_* for the spheroidal component of local galaxies.

$$\log\left(M_{BH}/M_\odot\right) = \alpha + \beta \log\left(\sigma_*/\sigma_0\right)$$

The $M_{BH} - \sigma_*$ relation

- Through the 1990s and early 2000s,
  - It became evident that essentially *all* galaxies and at least *some* GCs contain nuclear SMBHs.
  - The radio source Sag A^* near the center of the MW was found to be associated with a $\sim 10^6 M_\odot$ SMBH.
  - Ferrarese & Merritt and Gebhardt et al. discovered a (relatively) tight relationship between M_{BH} and central σ_* for the spheroidal component of local galaxies.

$$\log\left(M_{BH}/M_\odot\right) = \alpha + \beta \log\left(\sigma_*/\sigma_0\right)$$

A careful review by Tremaine et al. 2002, based on observations of 31 local galaxies, found

$$\alpha = 8.13 \pm 0.06, \qquad \beta = 4.02 \pm 0.32, \qquad \text{where } \sigma_0 = 200 \text{ km/s}$$

Summary plot from Tremaine et al. 2002

- ○, ● masses determined from stellar kinematics.
- △ masses determined from gas kinematics.
- $*$ masses determined from maser kinematics.
- ● masses from Gebhardt et al.
- - - 1 σ limit on best fit.

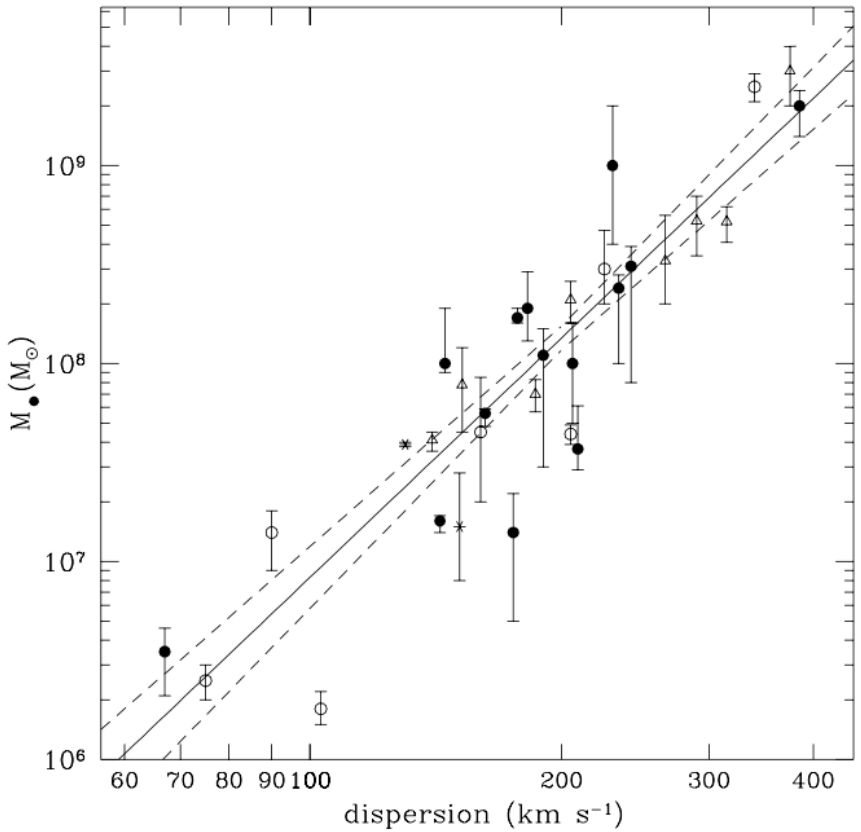

Implications of the $M_{BH} - \sigma_*$ relation

What causes M_{BH} and σ_* to be related?

Some possibilities:

- The SMBH and bulge form in the same potential well. They share an environment and history.
- The SMBH and bulge interact through feedback in such a way as to produce the relation.
- A combination of these.

Implications of the $M_{BH} - \sigma_*$ relation

What causes M_{BH} and σ_* to be related?

Some possibilities:

- The SMBH and bulge form in the same potential well. They share an environment and history.
- The SMBH and bulge interact through feedback in such a way as to produce the relation.
- A combination of these.

Analytic and numerical models successfully reproduce the relation using **different** assumptions.

Models disagree as to the evolution of the relation with cosmological time.

Implications and Evolution of $M_{BH} - \sigma_*$

Depending on the assumed initial conditions and the feedback mechanism used, there are three broad possibilities:

For a fixed value of σ_*,

1. M_{BH} increases with redshift; black holes develop more rapidly than spheroids at early times.

Implications and Evolution of $M_{BH} - \sigma_*$

Depending on the assumed initial conditions and the feedback mechanism used, there are three broad possibilities:

For a fixed value of σ_*,

1. M_{BH} increases with redshift; black holes develop more rapidly than spheroids at early times.
2. M_{BH} decreases with redshift; spheroids initially grow more rapidly than black holes.

Implications and Evolution of $M_{BH} - \sigma_*$

Depending on the assumed initial conditions and the feedback mechanism used, there are three broad possibilities:

For a fixed value of σ_*,

1. M_{BH} increases with redshift; black holes develop more rapidly than spheroids at early times.
2. M_{BH} decreases with redshift; spheroids initially grow more rapidly than black holes.
3. M_{BH} is independent of redshift; the mechanisms which set the relation act very quickly.

Implications and Evolution of $M_{BH} - \sigma_*$

Depending on the assumed initial conditions and the feedback mechanism used, there are three broad possibilities:

For a fixed value of σ_*,

1. M_{BH} increases with redshift; black holes develop more rapidly than spheroids at early times.
2. M_{BH} decreases with redshift; spheroids initially grow more rapidly than black holes.
3. M_{BH} is independent of redshift; the mechanisms which set the relation act very quickly.

Note: Analyzing *deviations* from the local relation does not strongly constrain theoretical models...

Implications and Evolution of $M_{BH} - \sigma_*$

Recall:

$$\log\left(M_{BH}/M_{\odot}\right) = \alpha + \beta \log\left(\sigma_*/\sigma_0\right)$$

The normalization, α and the slope, β could independently vary with look-back time.

Implications and Evolution of $M_{BH} - \sigma_*$

Recall:

$$\log\left(M_{BH}/M_{\odot}\right) = \alpha + \beta \log\left(\sigma_*/\sigma_0\right)$$

The normalization, α and the slope, β could independently vary with look-back time.

$\therefore$ Properly testing the evolution of $M_{BH} - \sigma_*$ requires the analysis of samples of galaxies in several narrow redshift bins. Otherwise, there could be degeneracies.

Depending on the evolution of α and β, certain hypotheses could be discarded. For instance, models employing thermal AGN feedback predict that α evolves with time, while β is independent of time.

Observed M_{BH} Evolution

Woo, et al. (2006,2008) have measured M_{BH} and σ_* for galaxies at $z \approx 0.36$ and $z \approx 0.57$ with fairly low-luminosity AGN.

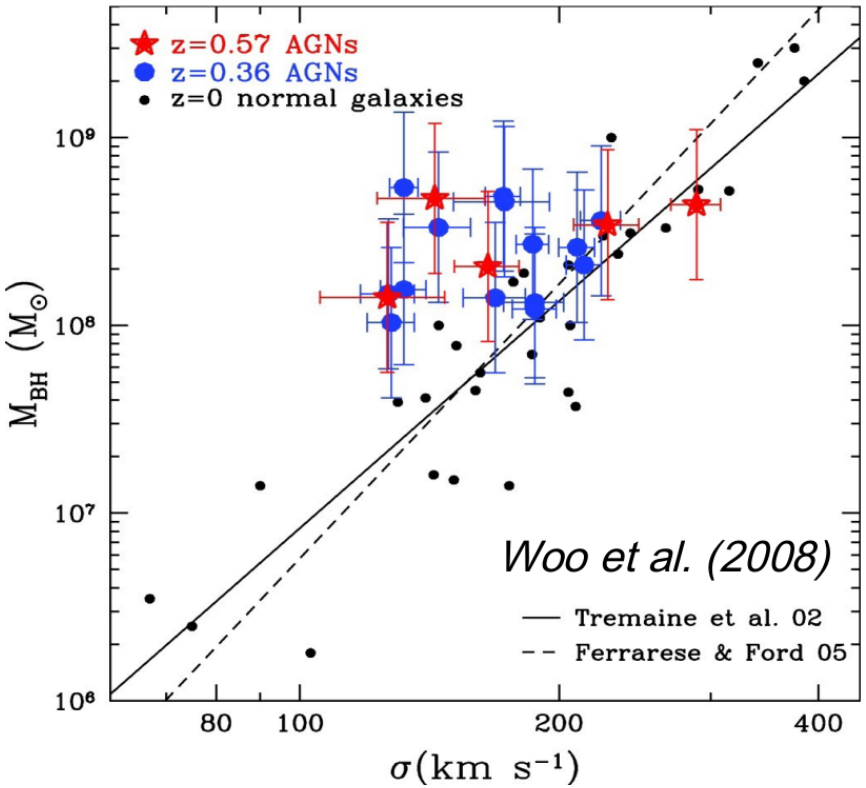

- Sample sizes were too small to determine α or β.
- For fixed σ_*, M_{BH} is larger.
- A similar result was found by Shields et al., 2006.
- Is this just because these are AGN hosts?

- Bennert et al. (2010) performed a detailed analysis of nearby AGN host galaxies (with AGN dim enough to measure σ_*).
- Within the uncertainty, the local AGN relation agrees with local inactive galaxy relation, but has somewhat more scatter.

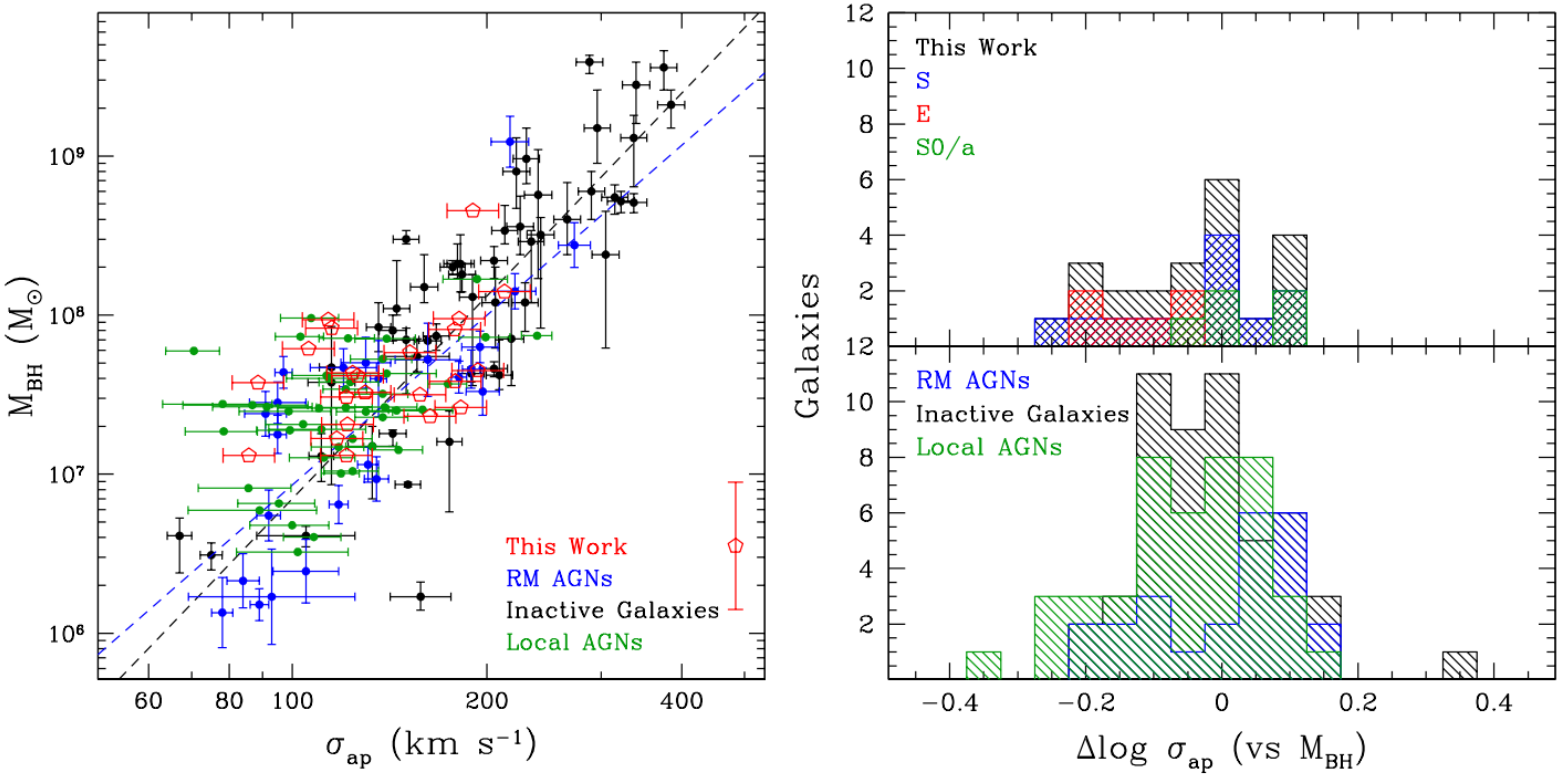

Increasing z and Sample Sizes

- The work of Woo et al. only employed low-luminosity AGN.
- Expanding the variety of objects and the redshift range would be beneficial.

Increasing z and Sample Sizes

- The work of Woo et al. only employed low-luminosity AGN.
- Expanding the variety of objects and the redshift range would be beneficial.
- Hiner and Canalizo have begun studying $M_{BH} - \sigma_*$ for a different class of objects: dust-reddened quasars.
  - The AGN appears to be significantly obscured by dust.
  - The stellar population seems to exhibit little or no dust-extinction.
  - Both σ_* and M_{BH} can be measured as far as $z \approx 1$
  - At least some of these objects appear to be remnants of recent mergers...

Uncertainties

- Observations of galaxies at $z > 0$ are needed in order to constrain galaxy formation and evolution models.
- Measuring M_{BH} for distant galaxies can only be done if there is an associated AGN.
- There is strong evidence that AGN are triggered by galaxy mergers.
- Galaxy mergers also trigger enhanced star formation episodes (starbursts).
- Star formation adds dust to the ISM.
- It is unclear how merger evolution and dust attenuation effect the measurement of σ_*...

Uncertainties

Previous $M_{BH} - \sigma_*$ simulation studies have done little to explain the evolution of σ_* during a merger:

- Simulators typically wait until galaxies have reached a steady state and *then* measure σ_* (300 Myr - 2 Gyr after final coalescence)

Uncertainties

Previous $M_{BH} - \sigma_*$ simulation studies have done little to explain the evolution of σ_* during a merger:

- Simulators typically wait until galaxies have reached a steady state and *then* measure σ_* (300 Myr - 2 Gyr after final coalescence)
- Simulators typically report the mean σ_* from ~ 100 projections of the merged system.

Uncertainties

Previous $M_{BH} - \sigma_*$ simulation studies have done little to explain the evolution of σ_* during a merger:

- Simulators typically wait until galaxies have reached a steady state and *then* measure σ_* (300 Myr - 2 Gyr after final coalescence)
- Simulators typically report the mean σ_* from ~ 100 projections of the merged system.
- To my knowledge, only one paper (Johansson et al., 2009) has documented the variation of the mean value of σ_* in high-resolution merger simulations.
  - The time resolution of measurements was low (200 Myr).
  - The anisotropy of the dispersion was not analyzed in depth.
  - The analysis placed more emphasis on the evolution of M_{BH}.

Some Uncertainties

- Simulators (T.J. Cox and K. Dasyra) have noted that σ_* can fluctuate significantly before reaching a steady value.
  - but they haven't published a detailed account!
- Because of the variations, galaxy modelers consider σ_* to be well-defined only for quiescent systems (just as temperature is only well-defined for systems in equilibrium)

Some Uncertainties

- Simulators (T.J. Cox and K. Dasyra) have noted that σ_* can fluctuate significantly before reaching a steady value.
  - but they haven't published a detailed account!
- Because of the variations, galaxy modelers consider σ_* to be well-defined only for quiescent systems (just as temperature is only well-defined for systems in equilibrium)

Meanwhile,

- Observers make measurements of σ_* for systems which have not relaxed to a steady state.
  - Thus far, there is no 100% reliable observational method of identifying the dynamical state.

Some Uncertainties

Furthermore,

- When measuring σ_* in simulations, the velocities of the star particles within the half-*mass* radius are used.
- Observers make flux-weighted measurements of σ_* using the light from the half-*light* radius.
- Dust extinction, and AGN contamination could cause the simulators' measurement of σ_* to differ from the observers' measurement.

Some Uncertainties

The impact of time-variation, anisotropy, and dust-extinction on measurements of σ_* has not yet been explored in depth.

My questions:

Some Uncertainties

The impact of time-variation, anisotropy, and dust-extinction on measurements of σ_* has not yet been explored in depth.

My questions:

- How significant are these effects?

Some Uncertainties

The impact of time-variation, anisotropy, and dust-extinction on measurements of σ_* has not yet been explored in depth.

My questions:

- How significant are these effects?
- Do these effects lead to random or systematic discrepancies in the measured vs. actual σ_*?

Some Uncertainties

The impact of time-variation, anisotropy, and dust-extinction on measurements of σ_* has not yet been explored in depth.

My questions:

- How significant are these effects?
- Do these effects lead to random or systematic discrepancies in the measured vs. actual σ_*?
- Are these effects responsible for some of the scatter observed in the $M_{BH} - \sigma_*$ relation?

Some Uncertainties

The impact of time-variation, anisotropy, and dust-extinction on measurements of σ_* has not yet been explored in depth.

My questions:

- How significant are these effects?
- Do these effects lead to random or systematic discrepancies in the measured vs. actual σ_*?
- Are these effects responsible for some of the scatter observed in the $M_{BH} - \sigma_*$ relation?
- Could understanding these effects allow observers to better interpret measurements of σ_*?

Outline

Section Overview

- Project goals
- Brief description of the code
- Brief description of the simulations
- Summary of results

Project Goals

- To examine the **evolution** of σ_* with time during dissipationless mergers.

Project Goals

- To examine the **evolution** of σ_* with time during dissipationless mergers.
- To examine the **directional dependence** of σ_* during and after dissipationless mergers.

Project Goals

- To examine the **evolution** of σ_* with time during dissipationless mergers.
- To examine the **directional dependence** of σ_* during and after dissipationless mergers.
- To study how an attenuating medium might influence flux-weighted σ_* measurements.

Project Goals

- To examine the **evolution** of σ_* with time during dissipationless mergers.
- To examine the **directional dependence** of σ_* during and after dissipationless mergers.
- To study how an attenuating medium might influence flux-weighted σ_* measurements.
- To become more fluent in C/C++.
- To gain the experience of writing an N-body simulation code.

Code Summary

Steps:

1. Input the size scale, D, number of star particles, N, and the number of stars per particle, n.

Code Summary

Steps:

1. Input the size scale, D, number of star particles, N, and the number of stars per particle, n.
2. Build stellar populations.
   i) Make an array of stellar masses $\mathcal{M}_j$ where the number of particles in each mass range is chosen in accordance with Kroupa IMF.

Code Summary

Steps:

1. Input the size scale, D, number of star particles, N, and the number of stars per particle, n.
2. Build stellar populations.
   i) Make an array of stellar masses $\mathcal{M}_j$ where the number of particles in each mass range is chosen in accordance with Kroupa IMF.
   ii) Build star particles by randomly choosing entries in $\mathcal{M}_j$.

Code Summary

Steps:

1. Input the size scale, D, number of star particles, N, and the number of stars per particle, n.
2. Build stellar populations.
   i) Make an array of stellar masses $\mathcal{M}_j$ where the number of particles in each mass range is chosen in accordance with Kroupa IMF.
   ii) Build star particles by randomly choosing entries in $\mathcal{M}_j$.
   iii) Restrict the maximum mass accepted (in order to age the stellar populations).

Code Summary

Steps:

1. Input the size scale, D, number of star particles, N, and the number of stars per particle, n.
2. Build stellar populations.
   i) Make an array of stellar masses $\mathcal{M}_j$ where the number of particles in each mass range is chosen in accordance with Kroupa IMF.
   ii) Build star particles by randomly choosing entries in $\mathcal{M}_j$.
   iii) Restrict the maximum mass accepted (in order to age the stellar populations).
   iv) Compute star particle luminosities, L_i, and masses, m_i,

$$L_i = \sum_j^n L_{ij}(M_{ij}) \qquad m_i = \sum_j^n M_{ij}$$

Code Summary

3. Compute the total mass of the system.

$$M = \sum_{i}^{N} m_i$$

Code Summary

3. Compute the total mass of the system.

$$M = \sum_{i}^{N} m_i$$

4. Construct a spheroidal stellar system.
   i) Randomly sample the Hernquist density profile.

$$\rho(r) = \frac{M}{2\pi} \frac{D}{r} \frac{1}{(r+D)^3}$$

Code Summary

3. Compute the total mass of the system.

$$M = \sum_{i}^{N} m_i$$

4. Construct a spheroidal stellar system.
   i) Randomly sample the Hernquist density profile.

$$\rho(r) = \frac{M}{2\pi} \frac{D}{r} \frac{1}{(r+D)^3}$$

   ii) Select speeds based on an approximation to the Virial theorem and use a uniform angular distribution for initial directions (Rather than using the Jeans equation)

Code Summary

3. Compute the total mass of the system.

$$M = \sum_{i}^{N} m_i$$

4. Construct a spheroidal stellar system.
   i) Randomly sample the Hernquist density profile.

$$\rho(r) = \frac{M}{2\pi}\frac{D}{r}\frac{1}{(r+D)^3}$$

   ii) Select speeds based on an approximation to the Virial theorem and use a uniform angular distribution for initial directions (Rather than using the Jeans equation)
   iii) Enforce $\mathbf{r}_{cm} = (0,0,0)$, $\mathbf{p}_{cm} = (0,0,0)$.

Code Summary

3. Compute the total mass of the system.

$$M = \sum_{i}^{N} m_i$$

4. Construct a spheroidal stellar system.
   i) Randomly sample the Hernquist density profile.

$$\rho(r) = \frac{M}{2\pi}\frac{D}{r}\frac{1}{(r+D)^3}$$

   ii) Select speeds based on an approximation to the Virial theorem and use a uniform angular distribution for initial directions (Rather than using the Jeans equation)
   iii) Enforce $\mathbf{r}_{cm} = (0,0,0)$, $\mathbf{p}_{cm} = (0,0,0)$.
5. Advance the particles forward in time for $\sim 2.5 t_{dyn}$ to allow the system to reach a steady, virialized state.

Animation: Collapse / Virialization

A 15.5K particle collapse simulation:

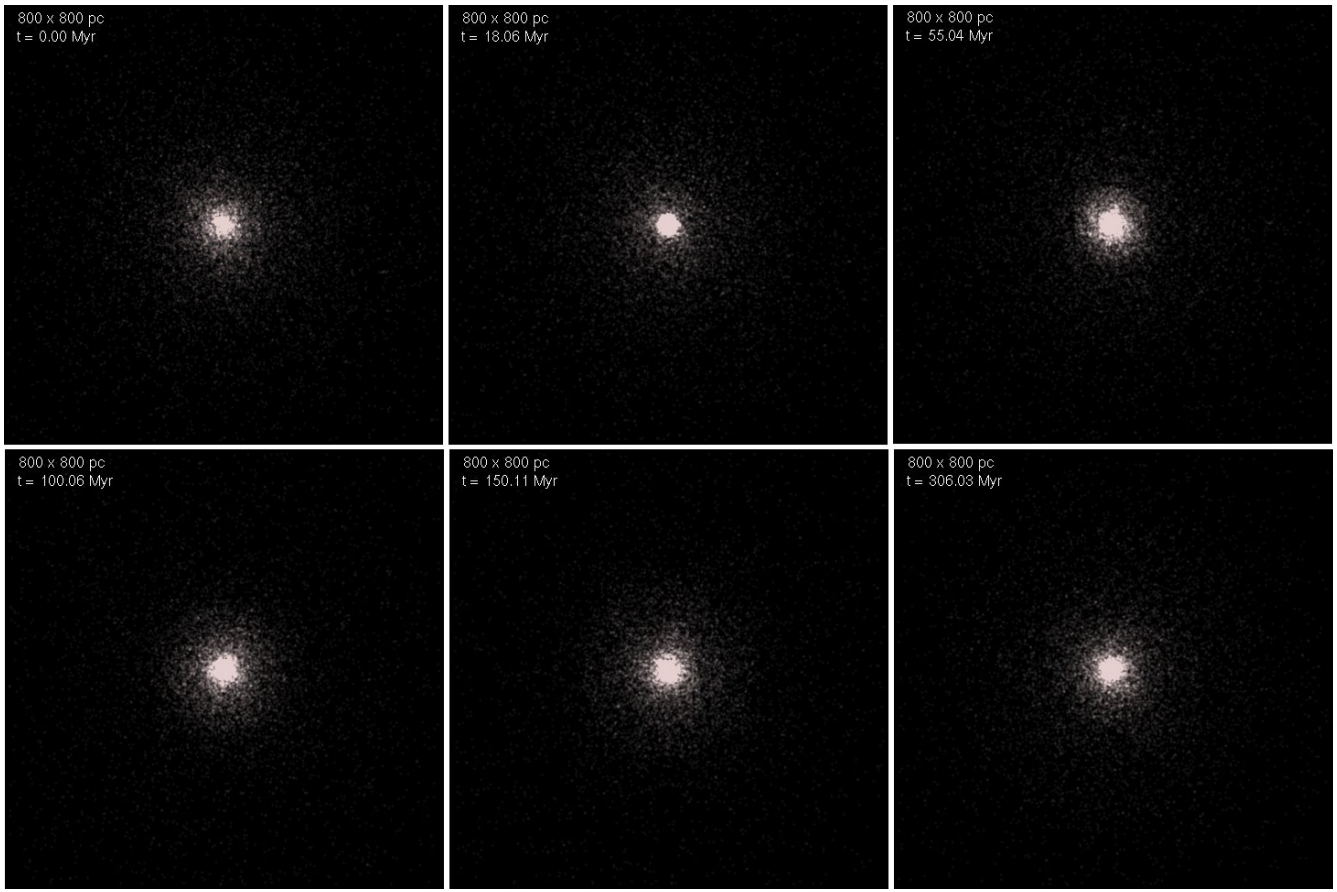

Code Summary

6. Collide two duplicate stellar systems.
   i) Clone the virialized system.

Code Summary

6. Collide two duplicate stellar systems.
   i) Clone the virialized system.
   ii) Use relative velocity and relative position vectors, $\mathbf{v}_{rel}$, $\mathbf{r}_{rel}$ to initialize the systems.

Code Summary

6. Collide two duplicate stellar systems.
   i) Clone the virialized system.
   ii) Use relative velocity and relative position vectors, $\mathbf{v}_{rel}$, $\mathbf{r}_{rel}$ to initialize the systems.
   iii) Evolve system forward in time.

Code Summary

6. Collide two duplicate stellar systems.
   i) Clone the virialized system.
   ii) Use relative velocity and relative position vectors, $\mathbf{v}_{rel}$, $\mathbf{r}_{rel}$ to initialize the systems.
   iii) Evolve system forward in time.
7. Run analysis routines at specified time interval.
   i) Assuming a gaussian PSF, create images of the system from $+x$, $+y$, $+z$, and specified arbitrary direction.

Code Summary

6. Collide two duplicate stellar systems.
   i) Clone the virialized system.
   ii) Use relative velocity and relative position vectors, $\mathbf{v}_{rel}$, $\mathbf{r}_{rel}$ to initialize the systems.
   iii) Evolve system forward in time.
7. Run analysis routines at specified time interval.
   i) Assuming a gaussian PSF, create images of the system from $+x$, $+y$, $+z$, and specified arbitrary direction.
   ii) Compute mass-weighted and flux-weighted σ_* from 150 random directions as well as the x,y,z directions.

Code Summary

6. Collide two duplicate stellar systems.
   i) Clone the virialized system.
   ii) Use relative velocity and relative position vectors, $\mathbf{v}_{rel}$, $\mathbf{r}_{rel}$ to initialize the systems.
   iii) Evolve system forward in time.
7. Run analysis routines at specified time interval.
   i) Assuming a gaussian PSF, create images of the system from $+x$, $+y$, $+z$, and specified arbitrary direction.
   ii) Compute mass-weighted and flux-weighted σ_* from 150 random directions as well as the x,y,z directions.
      a) Choose 150 random (θ, ϕ) uniformly distributed over sphere.

Code Summary

6. Collide two duplicate stellar systems.
   i) Clone the virialized system.
   ii) Use relative velocity and relative position vectors, $\mathbf{v}_{rel}$, $\mathbf{r}_{rel}$ to initialize the systems.
   iii) Evolve system forward in time.
7. Run analysis routines at specified time interval.
   i) Assuming a gaussian PSF, create images of the system from $+x$, $+y$, $+z$, and specified arbitrary direction.
   ii) Compute mass-weighted and flux-weighted σ_* from 150 random directions as well as the x,y,z directions.
      a) Choose 150 random (θ, ϕ) uniformly distributed over sphere.
      b) Rotate the system so that the viewing direction coincides with the z-axis. . .

Code Summary (analysis continued. . .)

c) Identify which star particles appear in the diffraction slit.

Code Summary (analysis continued. . .)

c) Identify which star particles appear in the diffraction slit.

d) Compute path lengths, d_i, through cylindrical attenuating slab of extinction coefficient, ε.

Code Summary (analysis continued. . .)

c) Identify which star particles appear in the diffraction slit.

d) Compute path lengths, d_i, through cylindrical attenuating slab of extinction coefficient, ε.

e) Compute flux contributions.

$$f_i = L_i e^{-\varepsilon d_i} \qquad \text{(no summation)}.$$

Code Summary (analysis continued. . .)

c) Identify which star particles appear in the diffraction slit.

d) Compute path lengths, d_i, through cylindrical attenuating slab of extinction coefficient, ε.

e) Compute flux contributions.

$$f_i = L_i e^{-\varepsilon d_i} \qquad \text{(no summation)}.$$

f) For each viewing direction, compute flux-weighted σ_*.

$$f\sigma_* = \sqrt{f_i v_i^2/F - (f_i v_i/F)^2} \qquad \text{where} \qquad F = \sum_i f_i$$

Code Summary (analysis continued. . .)

g) Compute mass-weighted σ_* for each viewing direction.

$$m\sigma_* = \sqrt{m_i v_i^2/\mathcal{M} - (m_i v_i/\mathcal{M})^2} \qquad \text{where} \qquad \mathcal{M} = \sum_i m_i$$

$$m\sigma_* \approx \sqrt{\langle v^2 \rangle - \langle v \rangle^2}$$

Code Summary (analysis continued. . .)

g) Compute mass-weighted σ_* for each viewing direction.

$$m\sigma_* = \sqrt{m_i v_i^2/\mathcal{M} - (m_i v_i/\mathcal{M})^2} \qquad \text{where} \qquad \mathcal{M} = \sum_i m_i$$

$$m\sigma_* \approx \sqrt{\langle v^2 \rangle - \langle v \rangle^2}$$

h) Compute directional max, min, mean, and std dev for $m\sigma_*$ and $f\sigma_*$.

Code Summary (analysis continued. . .)

g) Compute mass-weighted σ_* for each viewing direction.

$$m\sigma_* = \sqrt{m_i v_i^2/\mathcal{M} - (m_i v_i/\mathcal{M})^2} \qquad \text{where} \qquad \mathcal{M} = \sum_i m_i$$

$$m\sigma_* \approx \sqrt{\langle v^2 \rangle - \langle v \rangle^2}$$

h) Compute directional max, min, mean, and std dev for $m\sigma_*$ and $f\sigma_*$.

8. Save statistics to text file.
9. Save images.
10. Return to step 6.iii (advance forward)

Implementation

- Written in C++
- Parallelized with OpenMP
- Approx 1300 lines of code
- Libraries used:
  - Boost (ublas)
  - ImageMagick (Magick++)
  - OpenMP
- Post-processing of statistics: Python (numPy)
- Plotting: Python (matplotlib + TEX)
- Movies: FFmpeg automated with shell script

Collapse Analysis

Initial σ_*: 2.10 ± 0.03 km/s **Final** σ_*: 5.11 ± 0.09 km/s

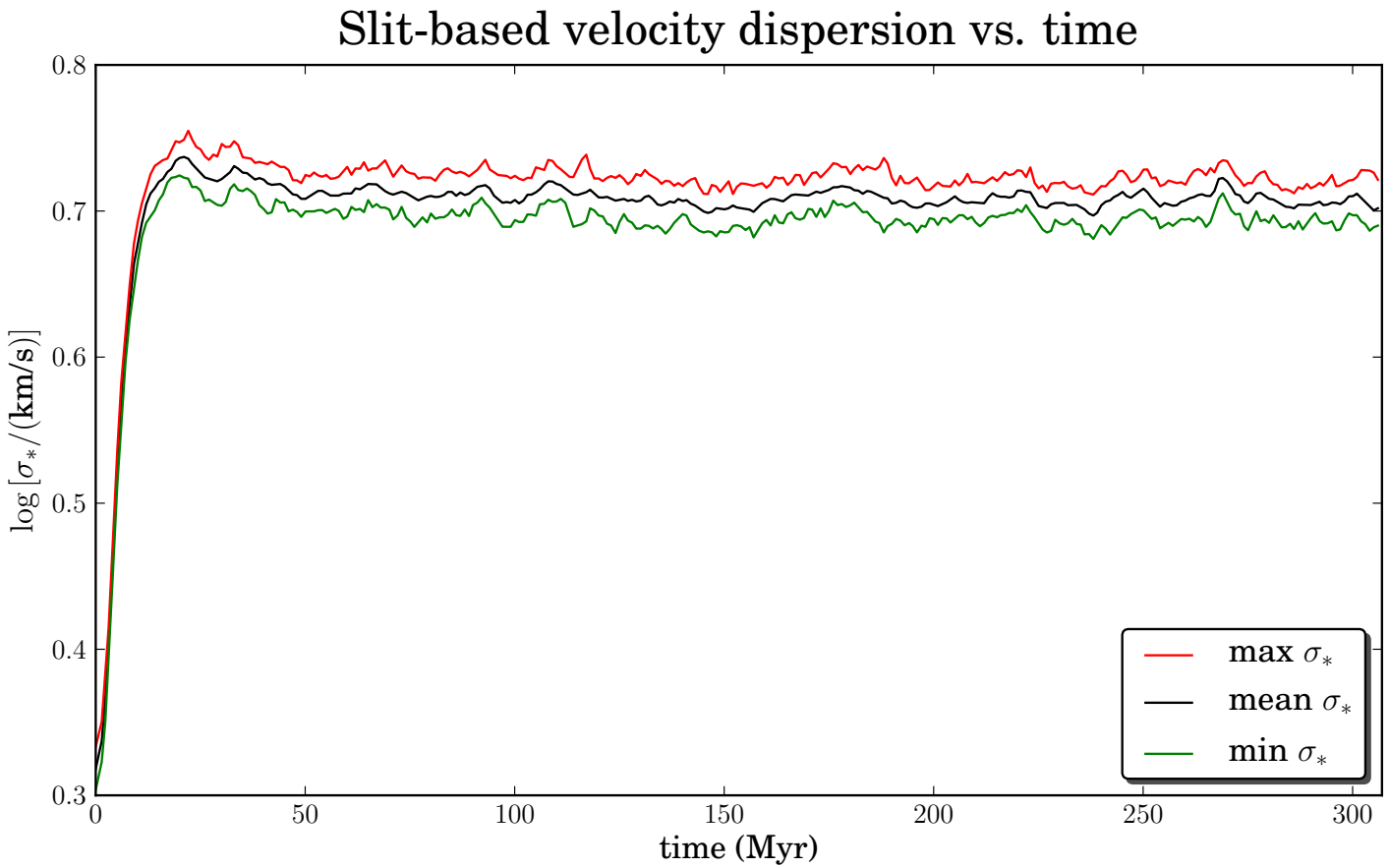

Collapse / Virialization Analysis

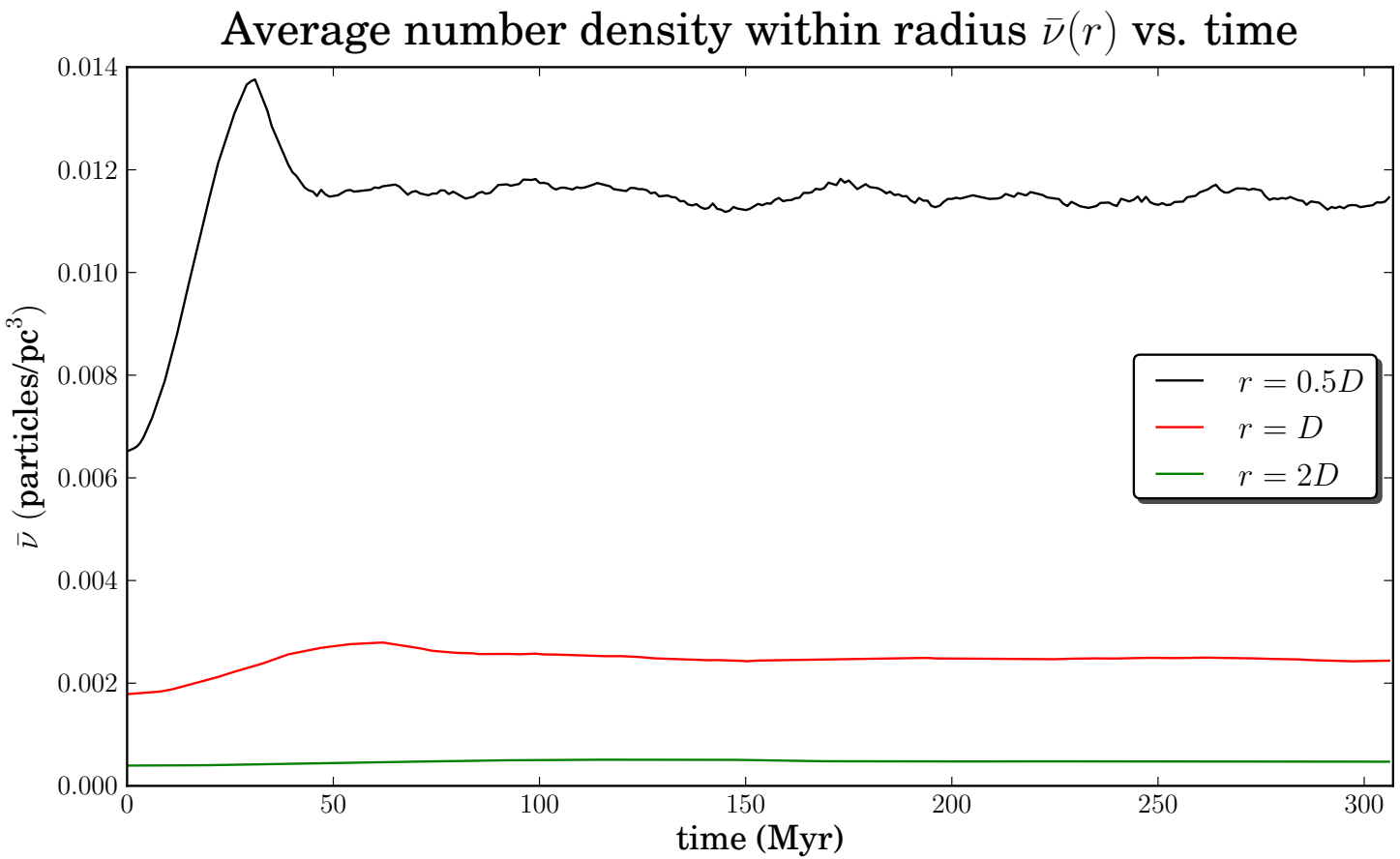

Initial Configurations

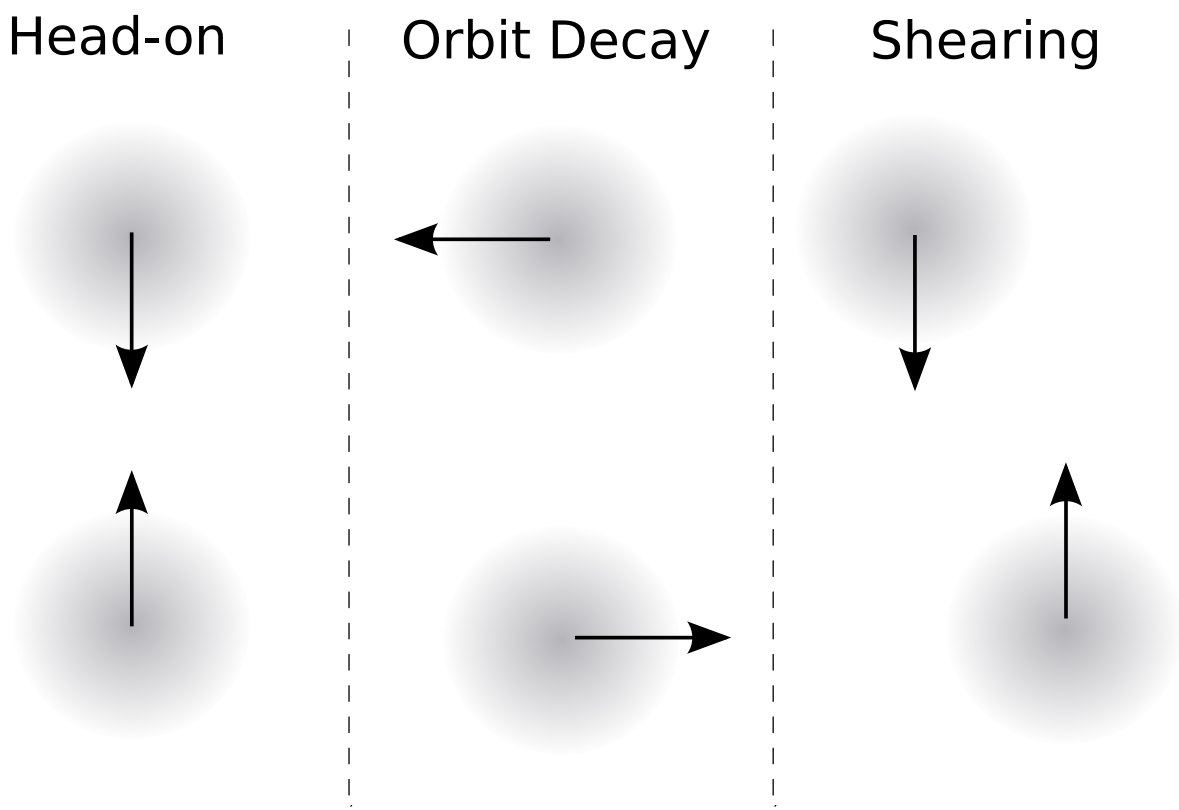

Head-on Collision

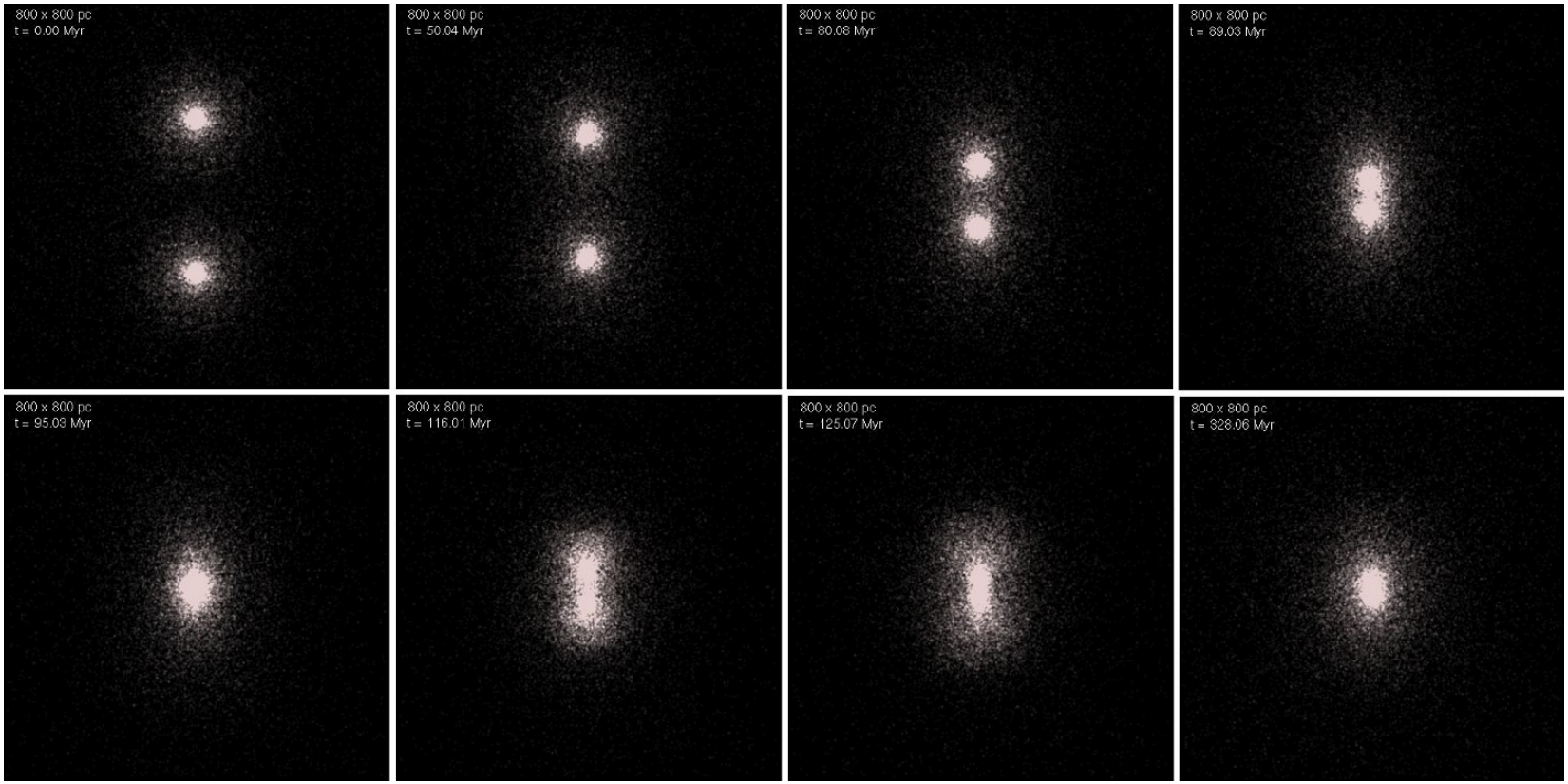

Head-on Collision Analysis

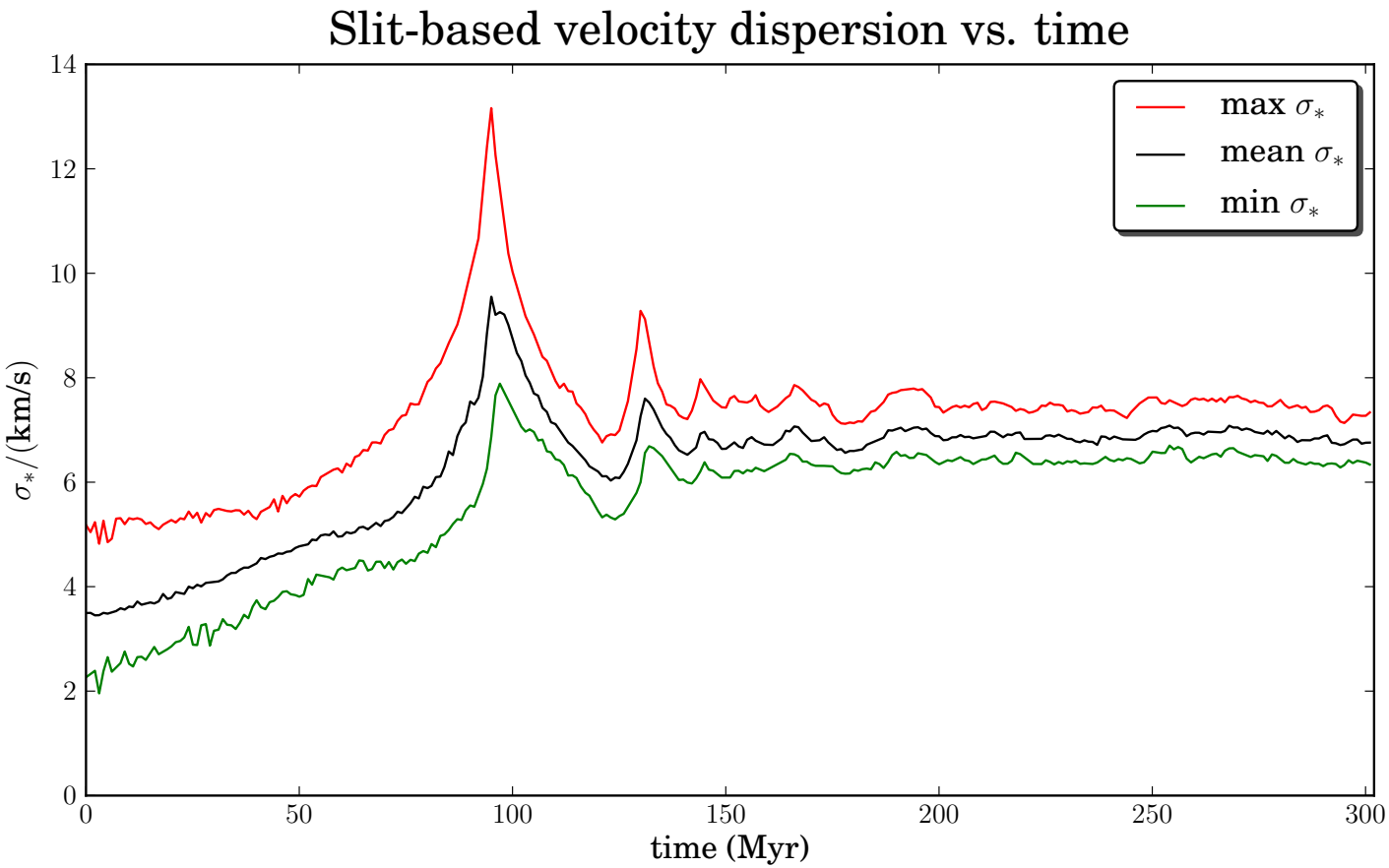

Head-on Collision Analysis

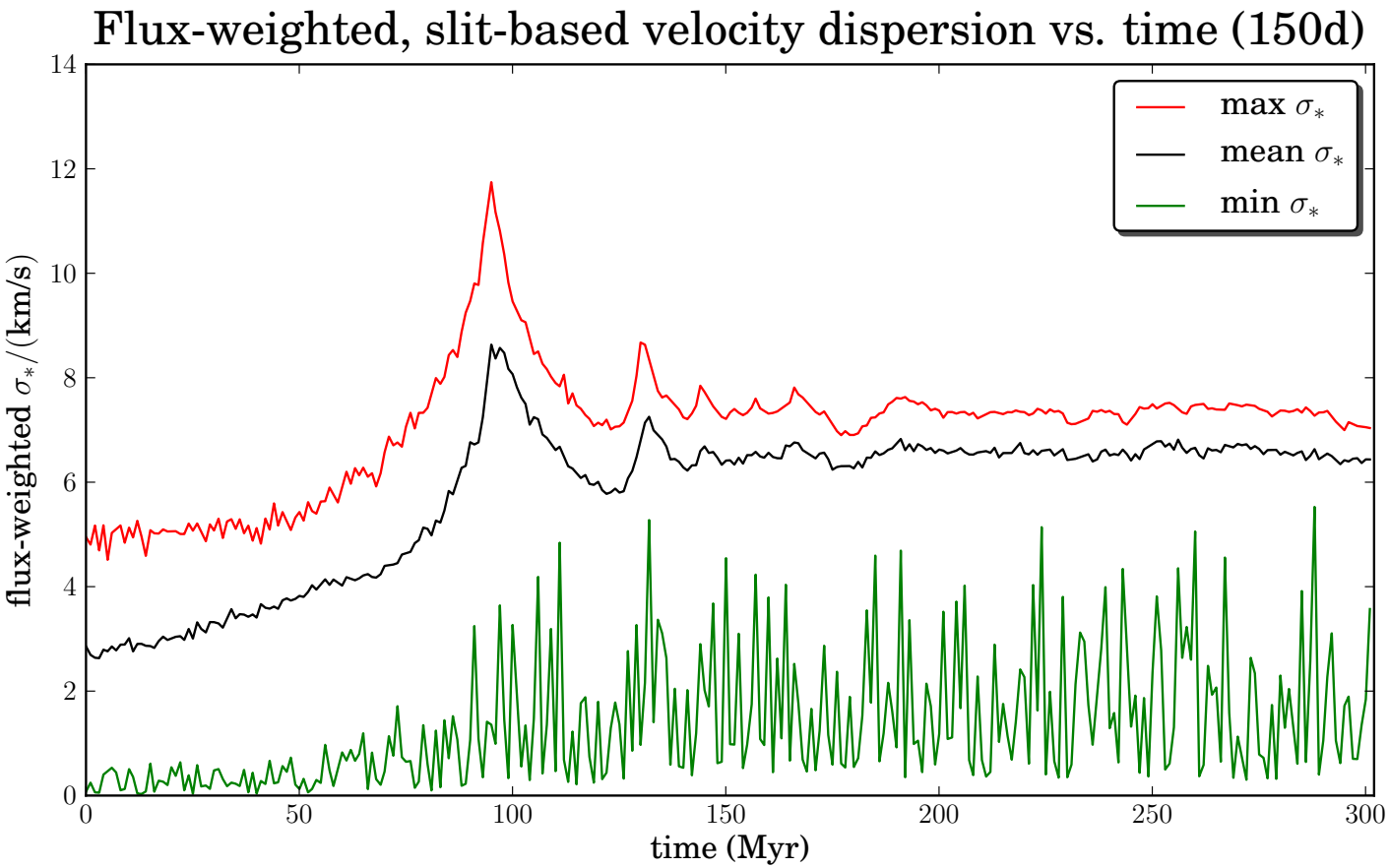

Head-on Collision Analysis

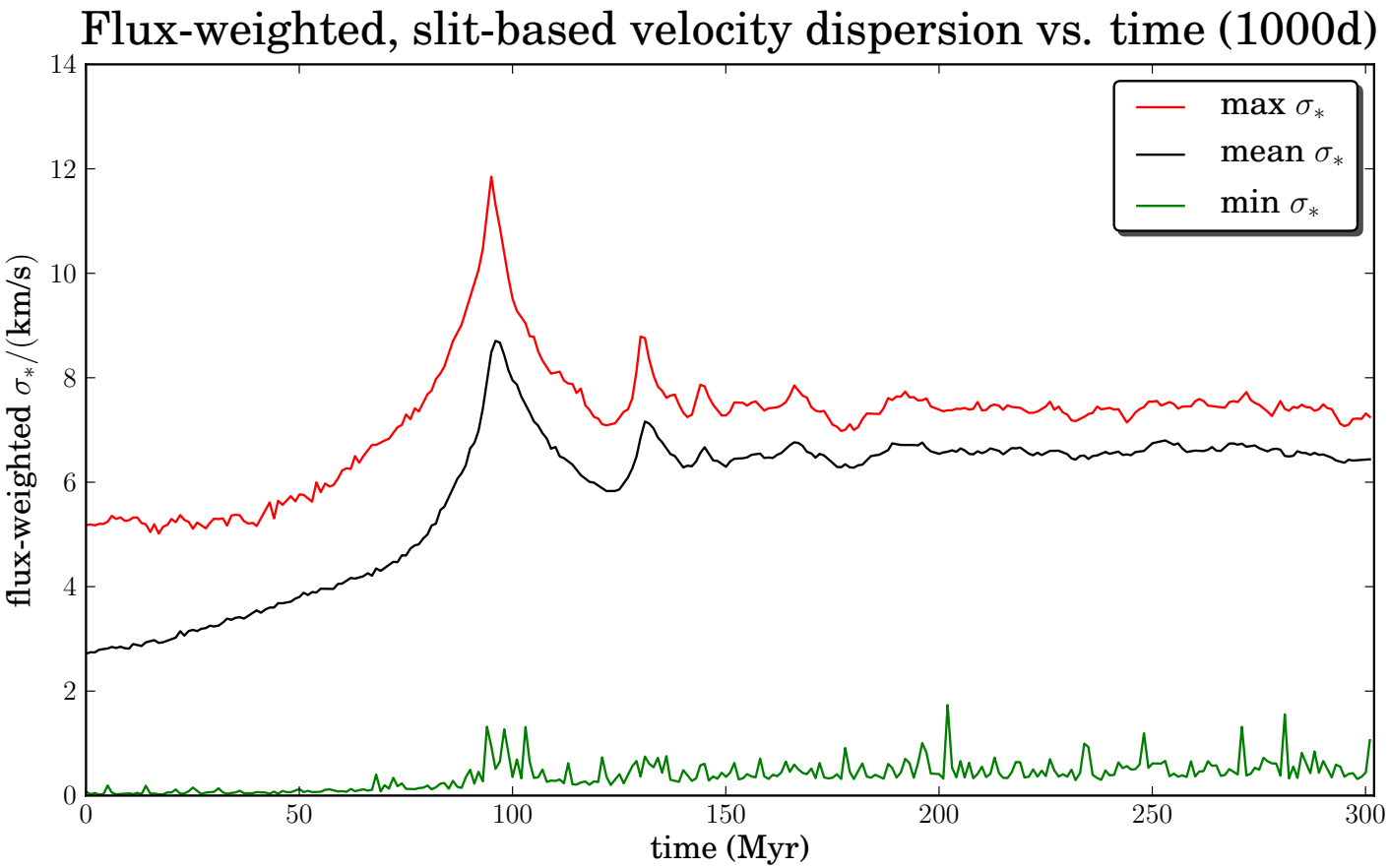

Head-on Collision Analysis

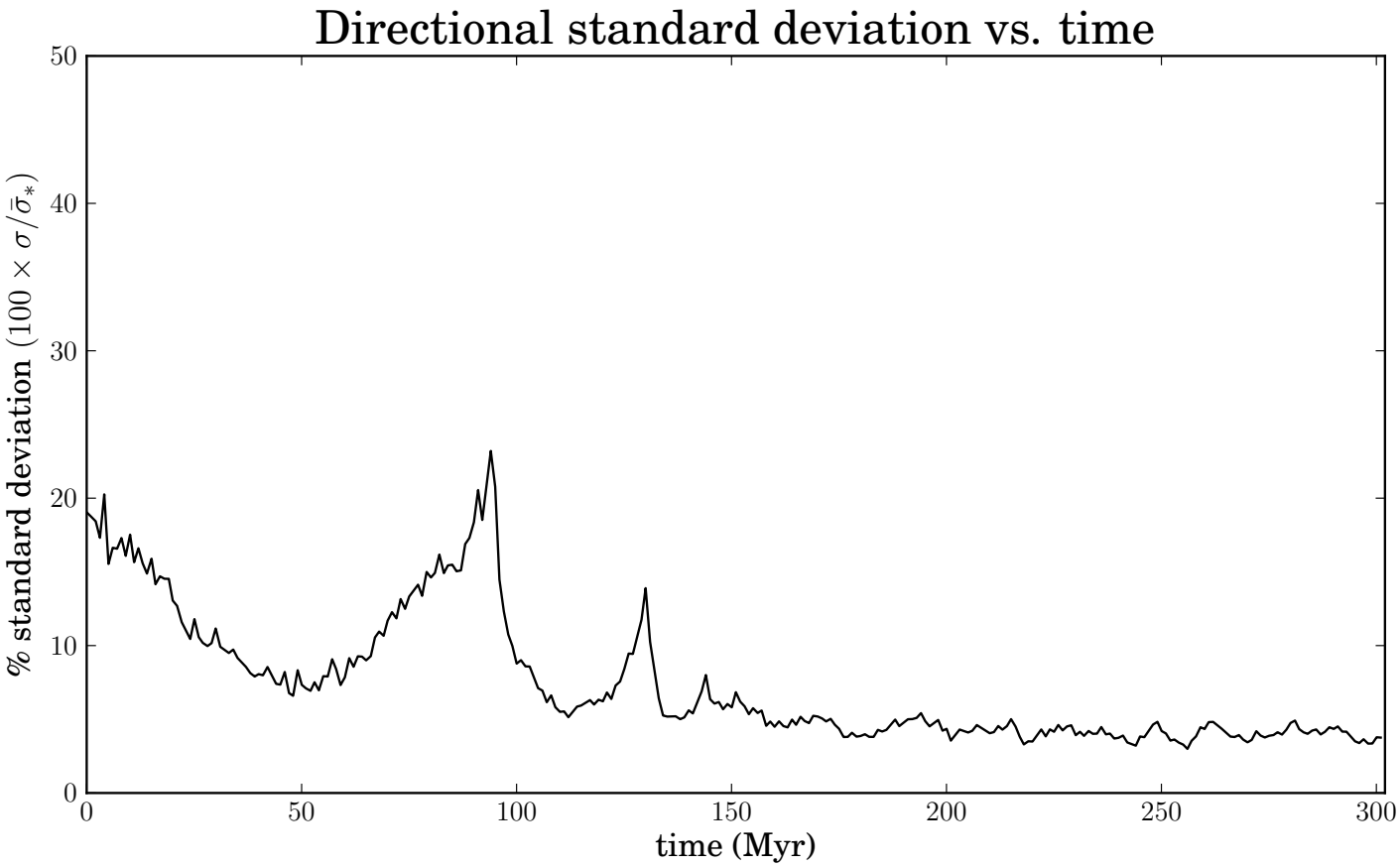

Head-on Collision Analysis

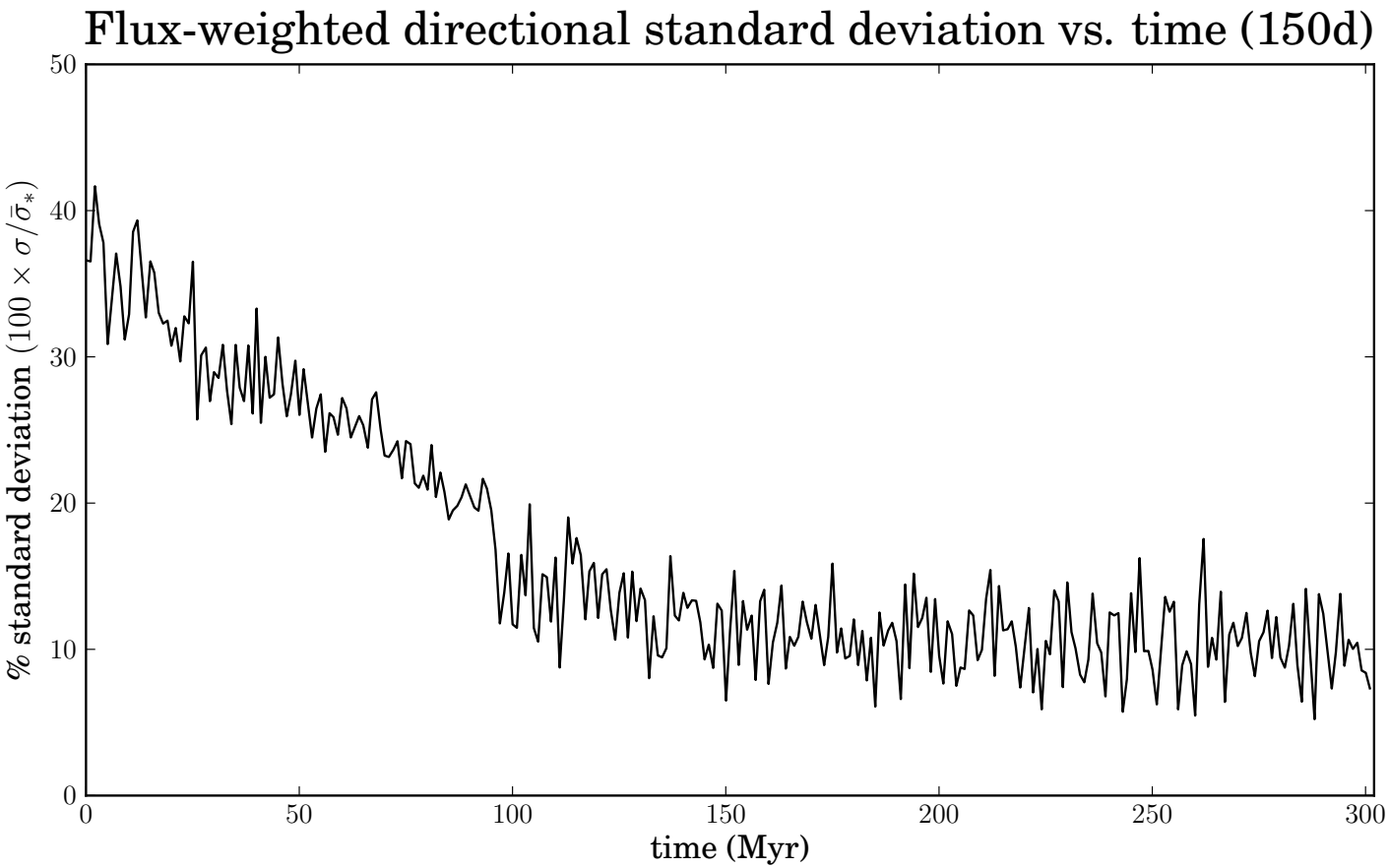

Head-on Collision Analysis

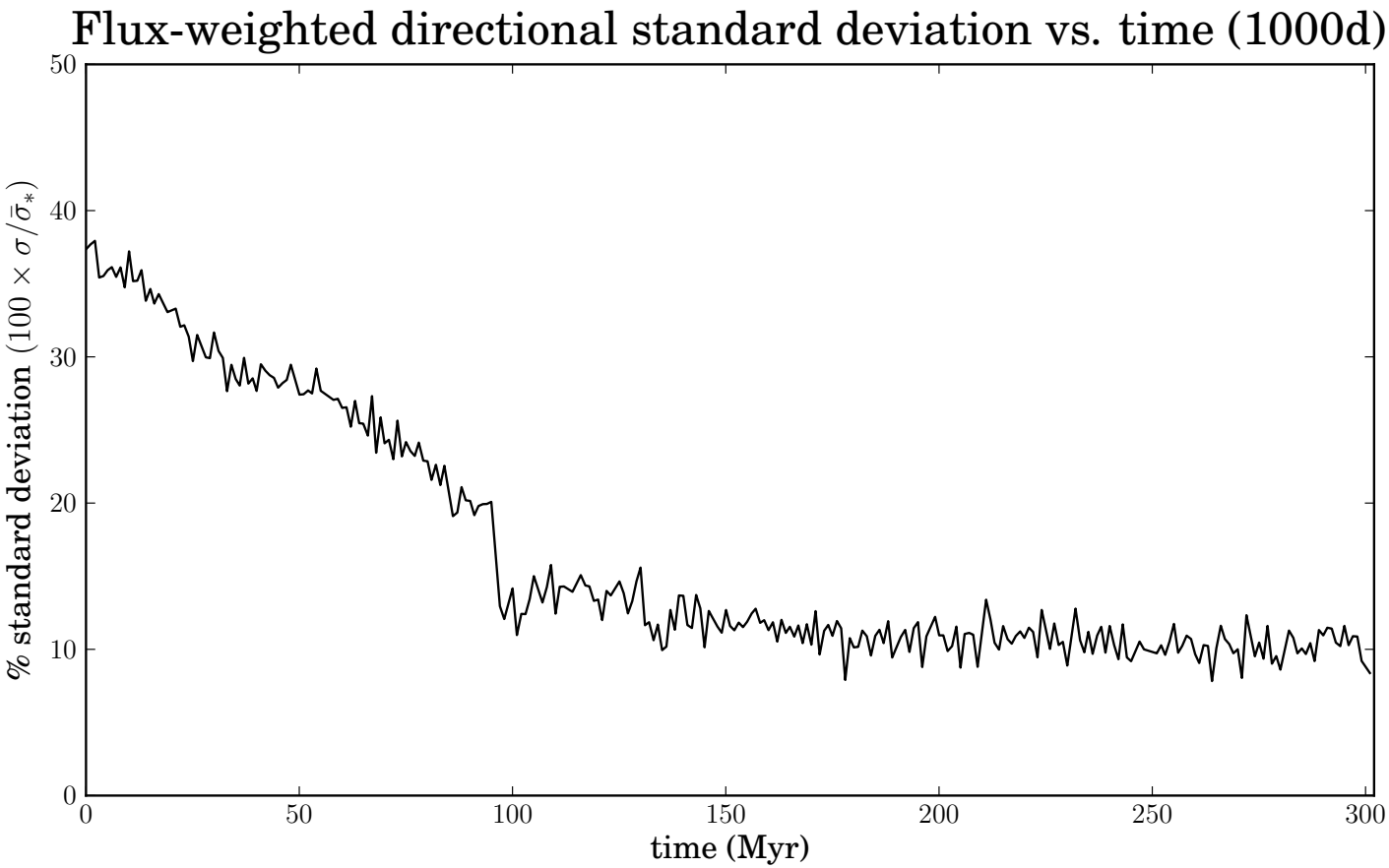

Head-on Collision Analysis

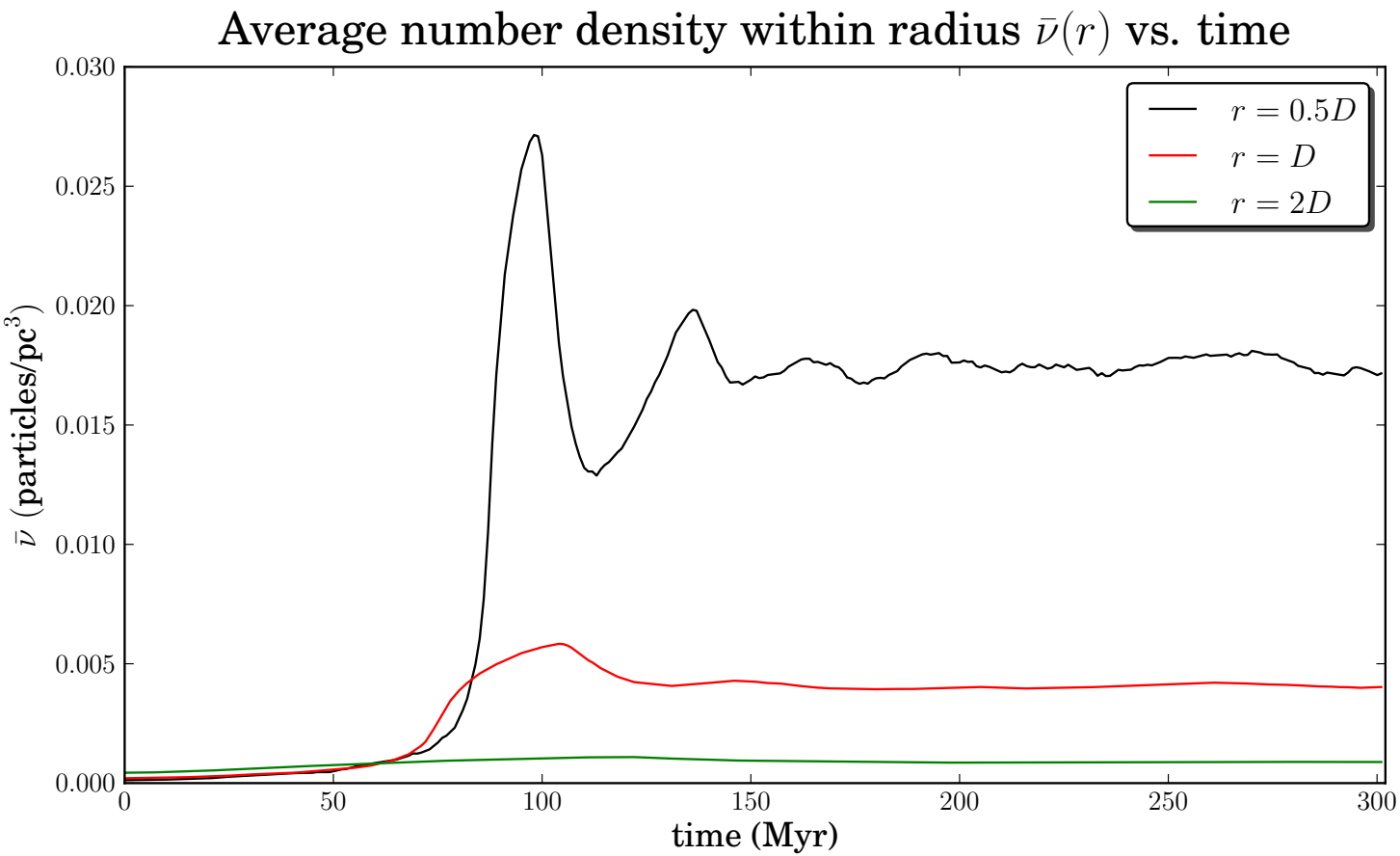

Head-on Collision Analysis

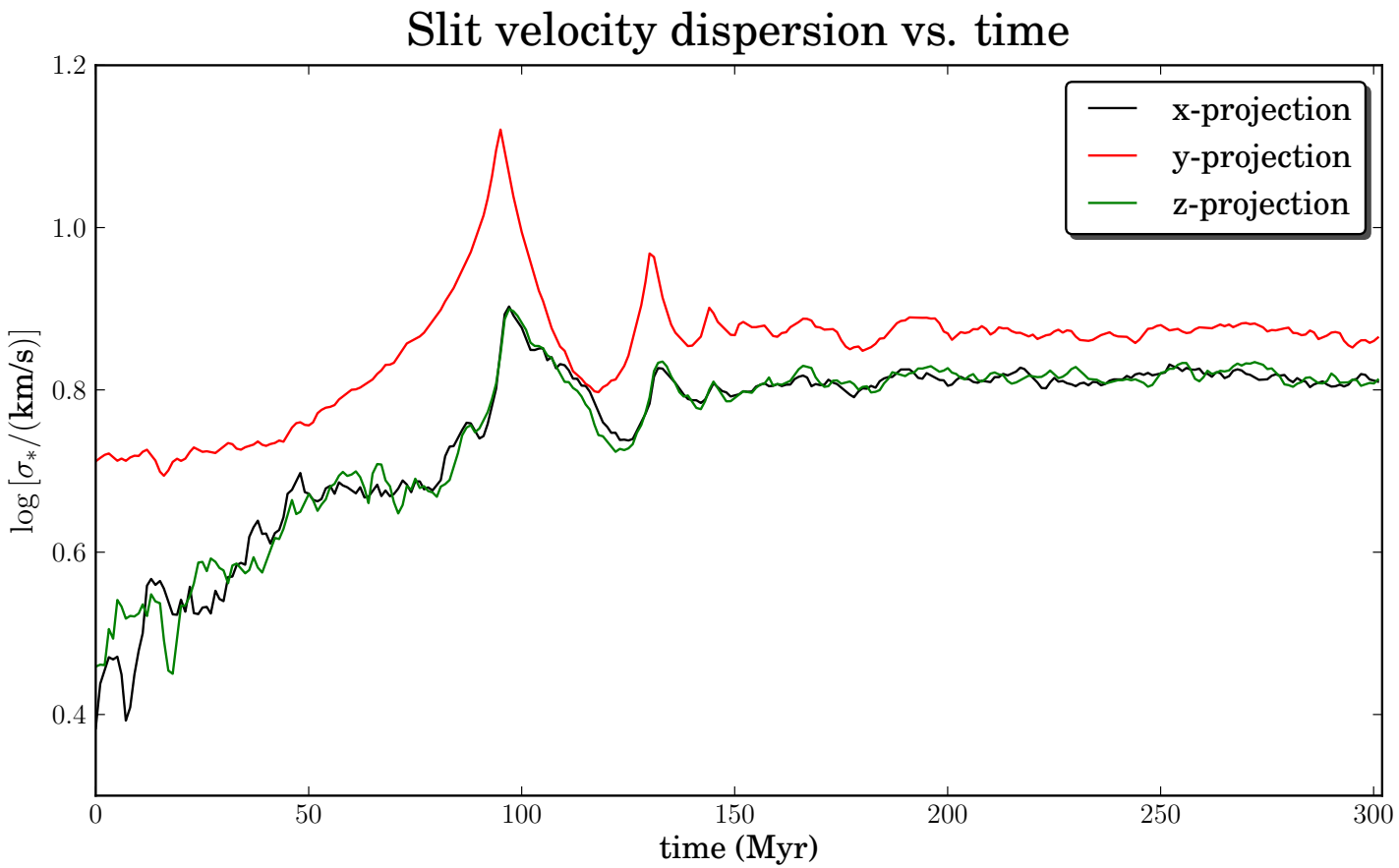

Orbit Decay

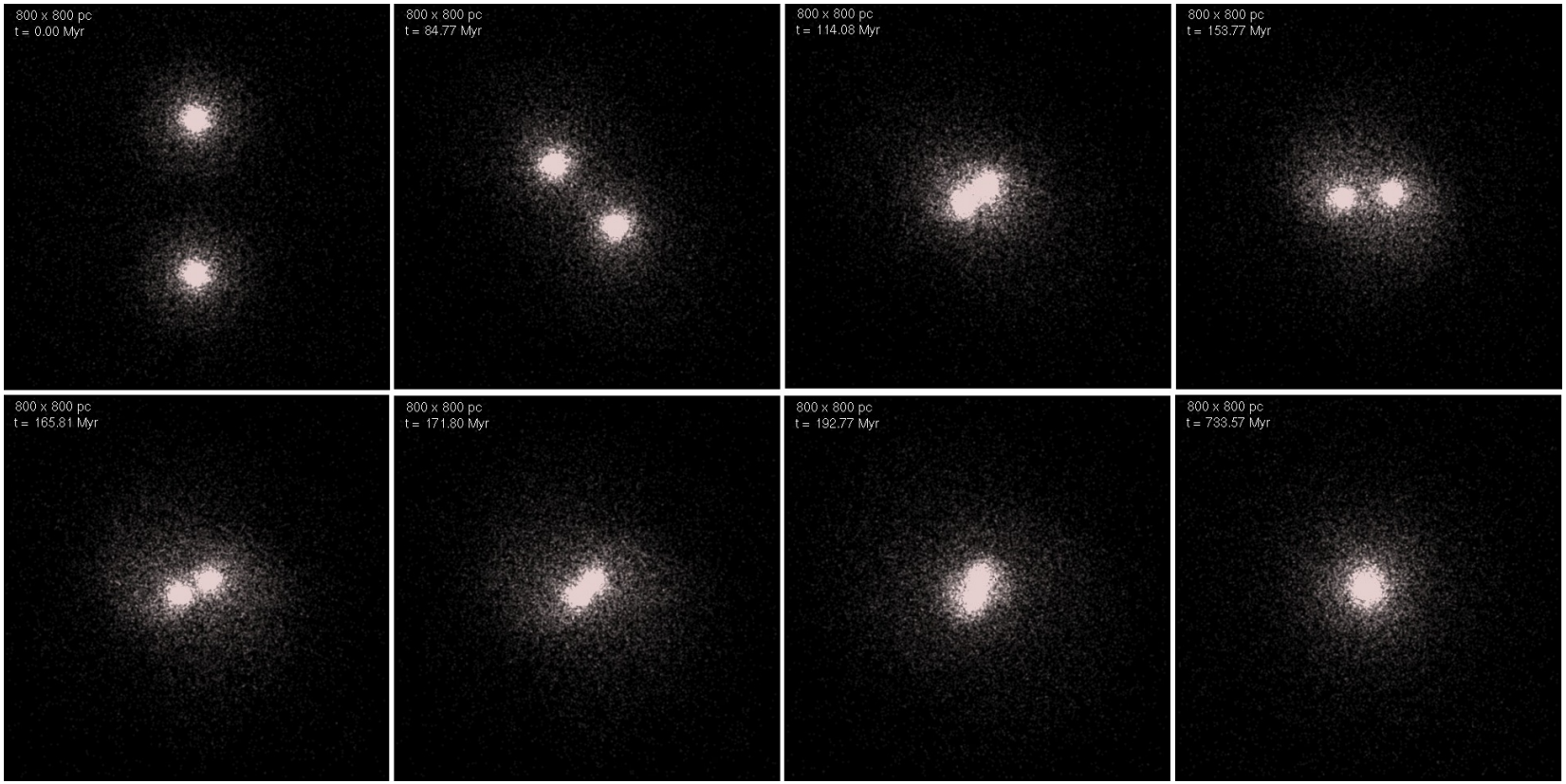
800 x 800 pc
t = 0.00 Myr
800 x 800 pc
t = 84.77 Myr
800 x 800 pc
t = 114.08 Myr
800 x 800 pc
t = 153.77 Myr
800 x 800 pc
t = 165.81 Myr
800 x 800 pc
t = 171.80 Myr
800 x 800 pc
t = 192.77 Myr
800 x 800 pc
t = 733.57 Myr

Orbit Decay Analysis

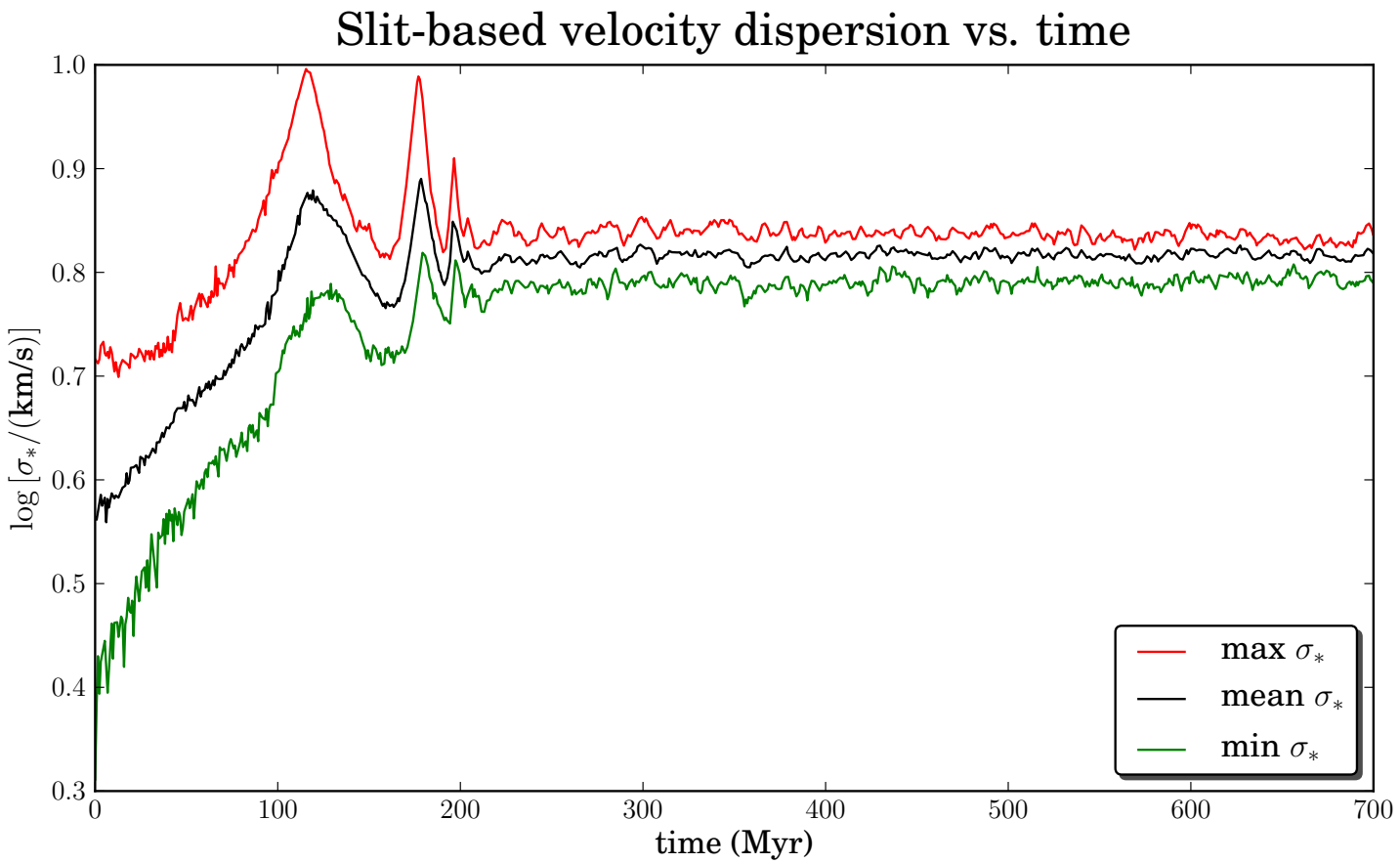

Orbit Decay Analysis

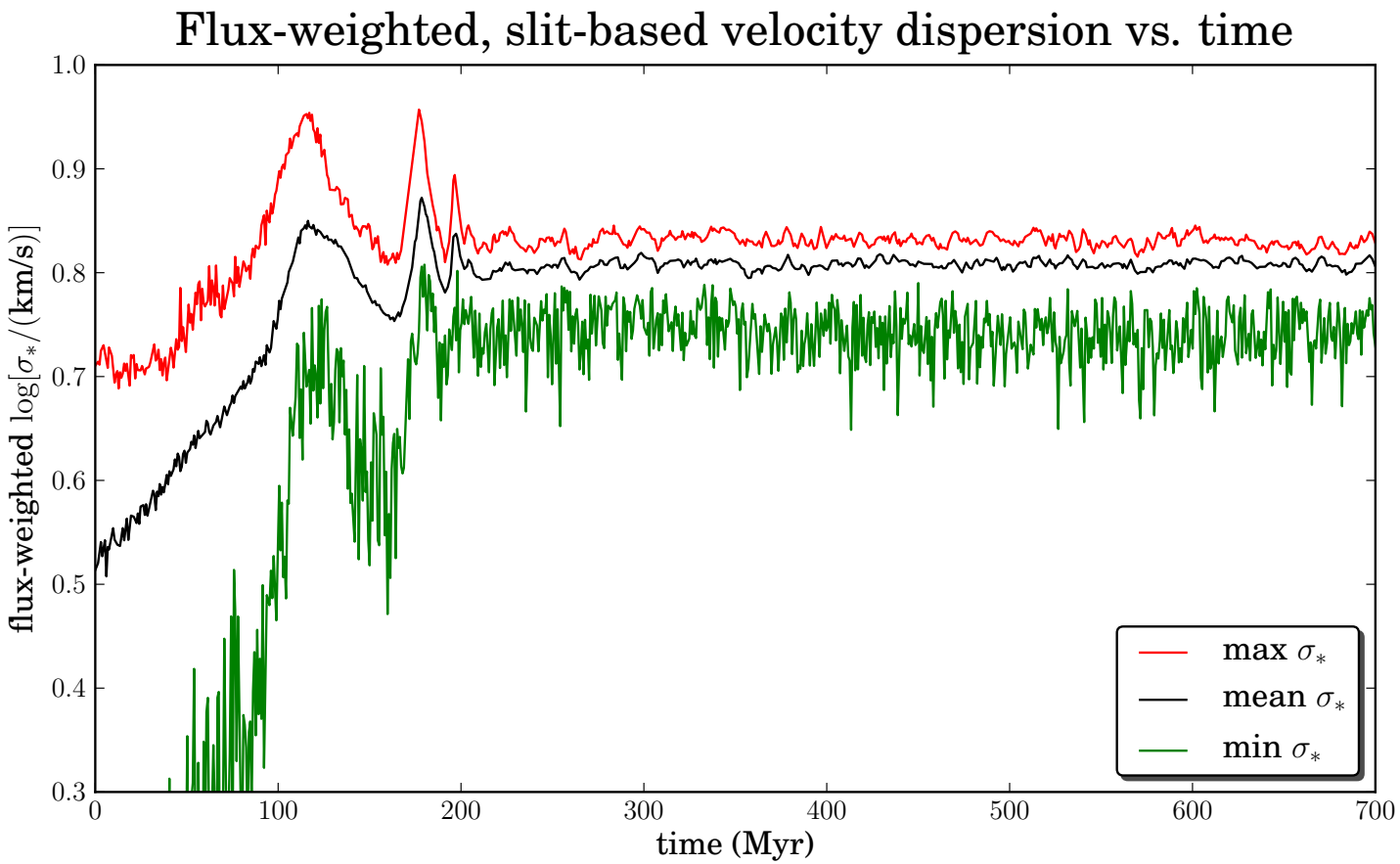

Orbit Decay Analysis

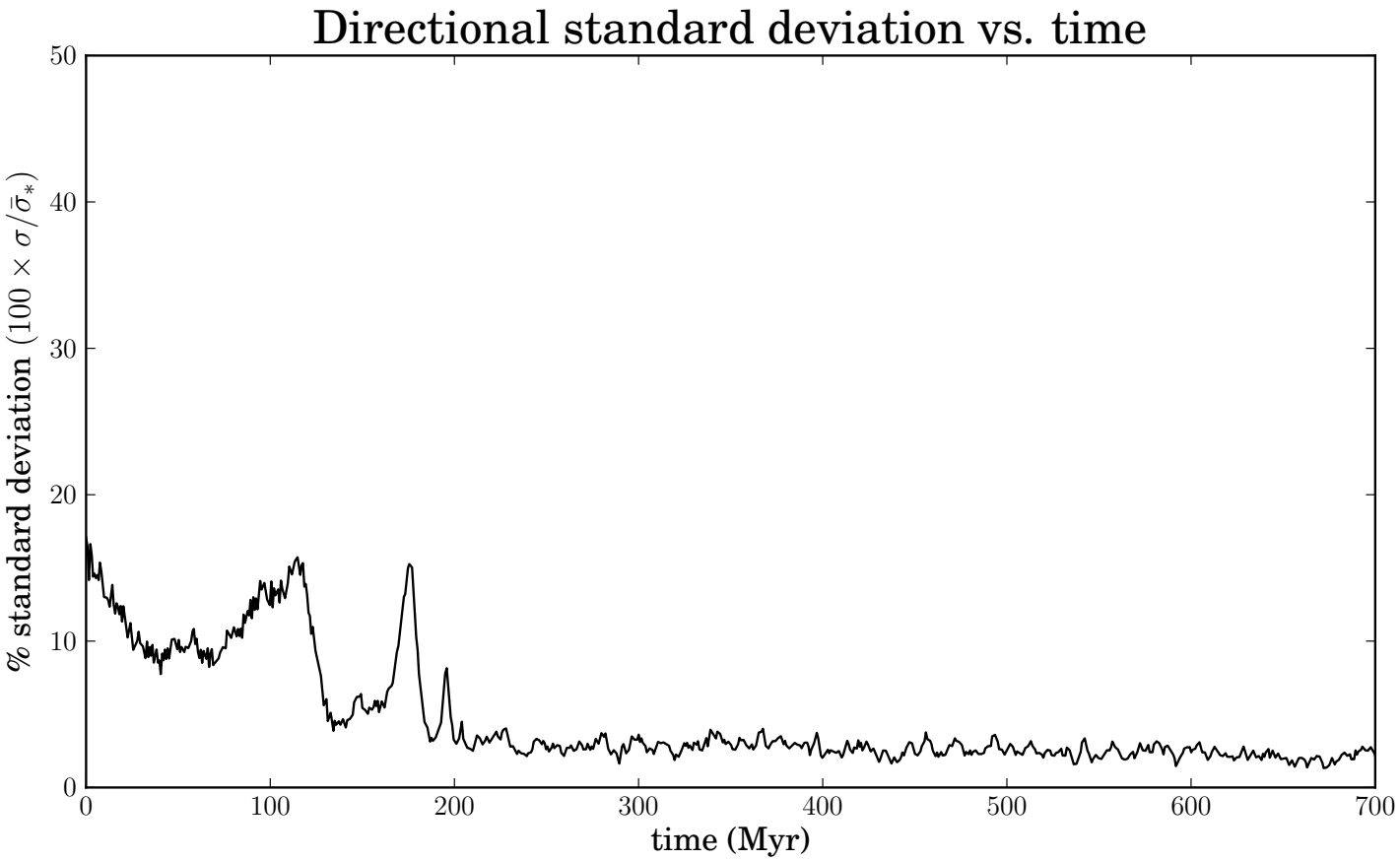

Orbit Decay Analysis

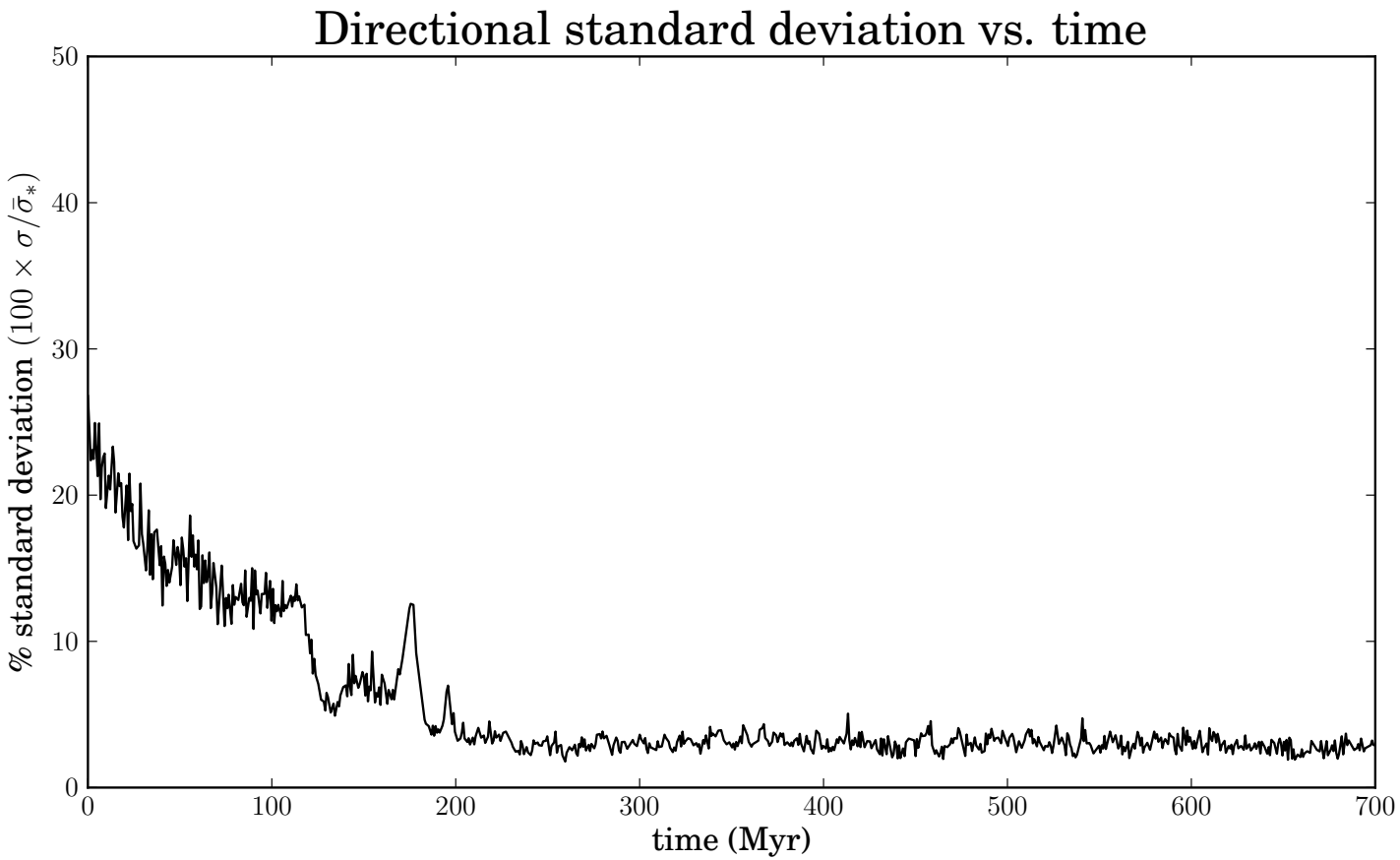

Orbit Decay Analysis

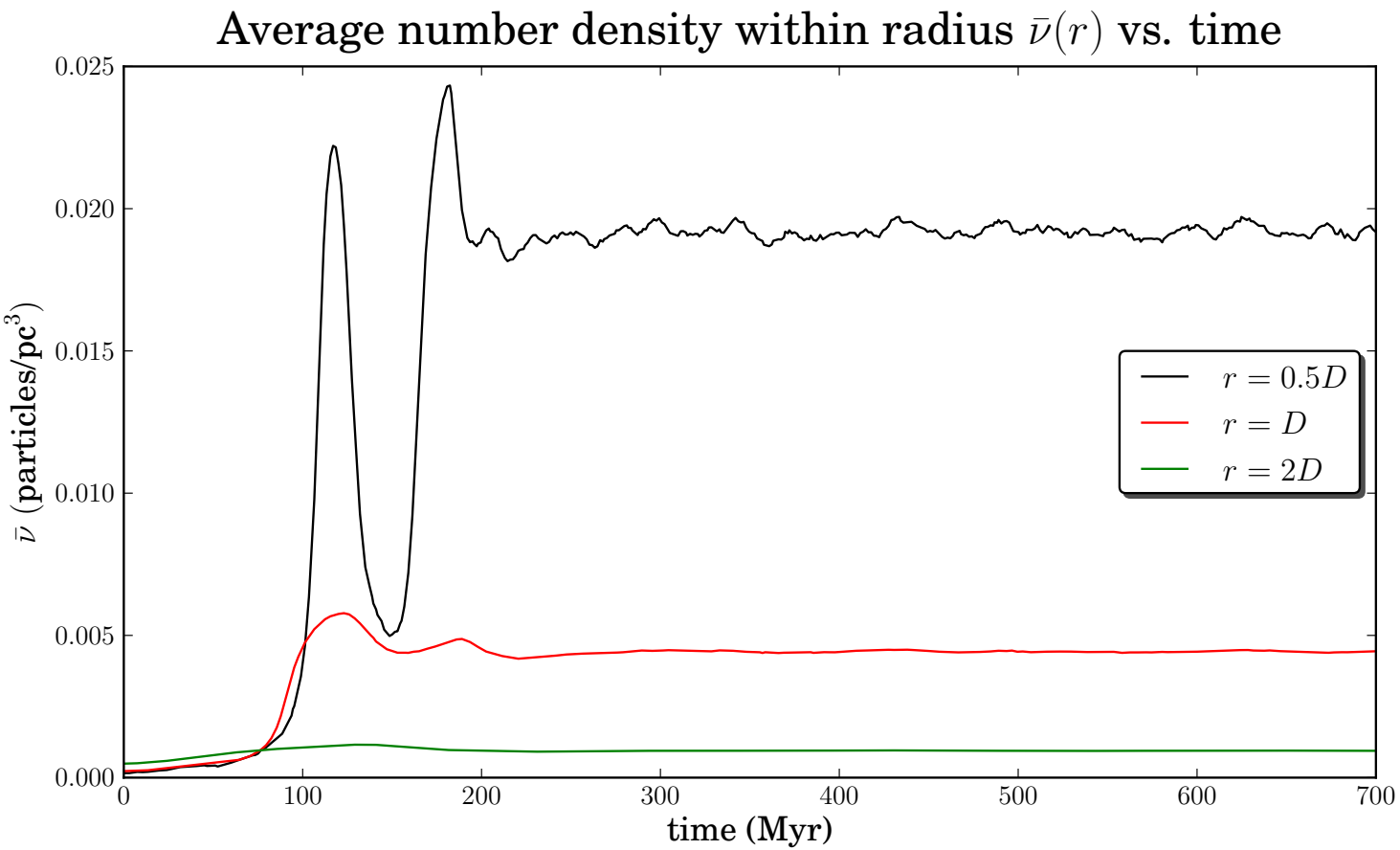

Orbit Decay Analysis

Rotation or dispersion?

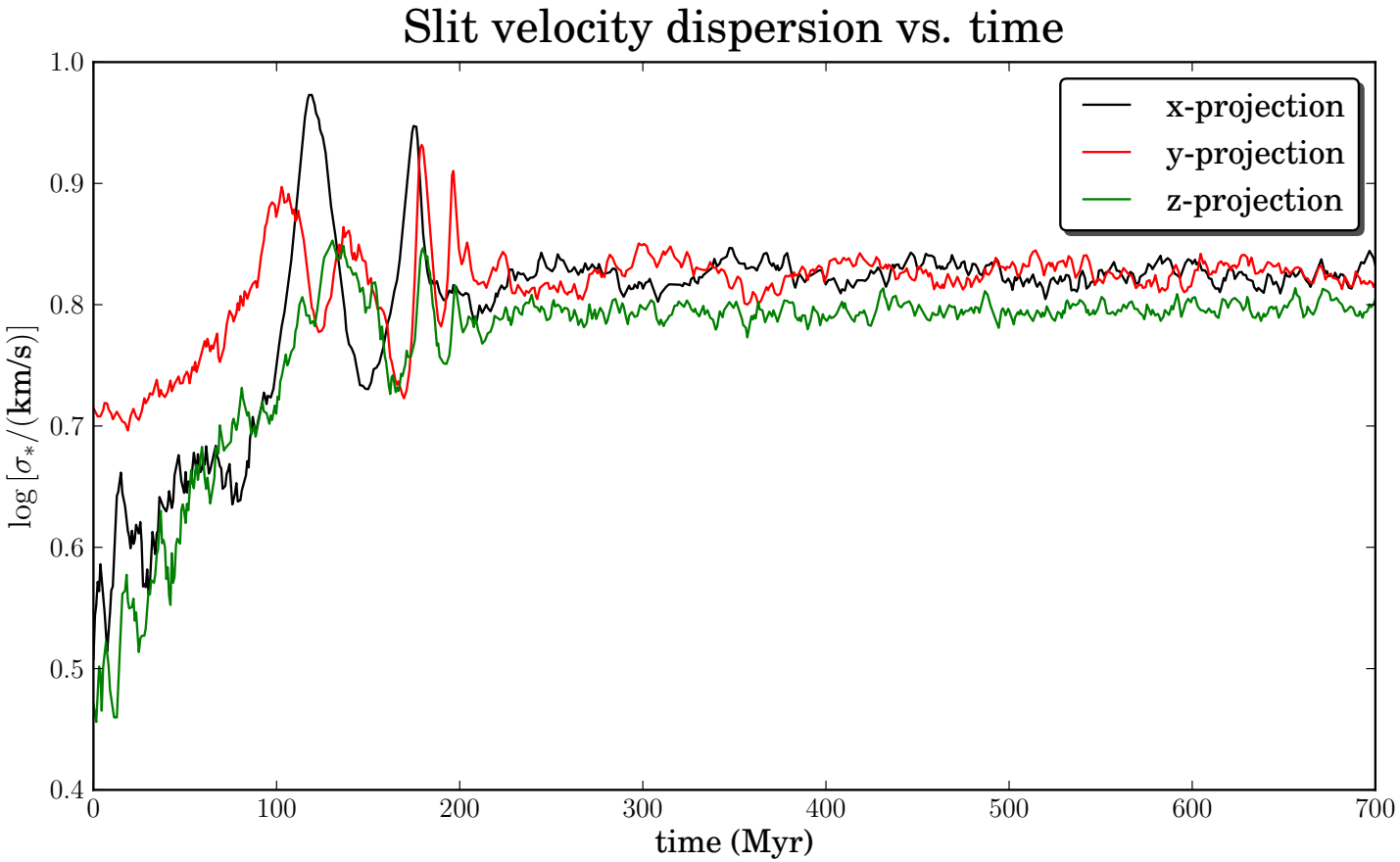

Shear

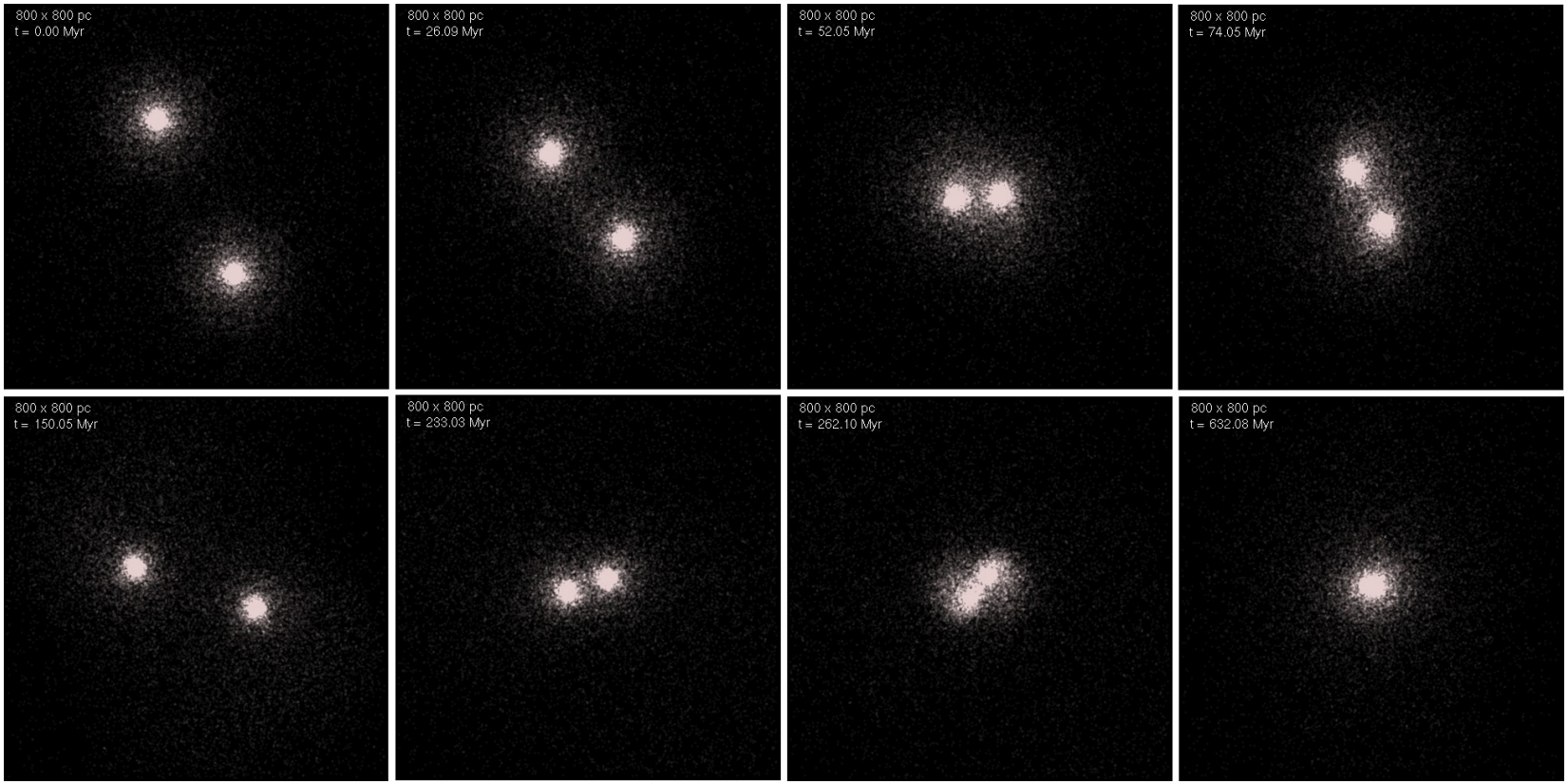
800 x 800 pc
t = 0.00 Myr
800 x 800 pc
t = 26.09 Myr
800 x 800 pc
t = 52.05 Myr
800 x 800 pc
t = 74.05 Myr
800 x 800 pc
t = 150.05 Myr
800 x 800 pc
t = 233.03 Myr
800 x 800 pc
t = 262.10 Myr
800 x 800 pc
t = 632.08 Myr

Shear Analysis

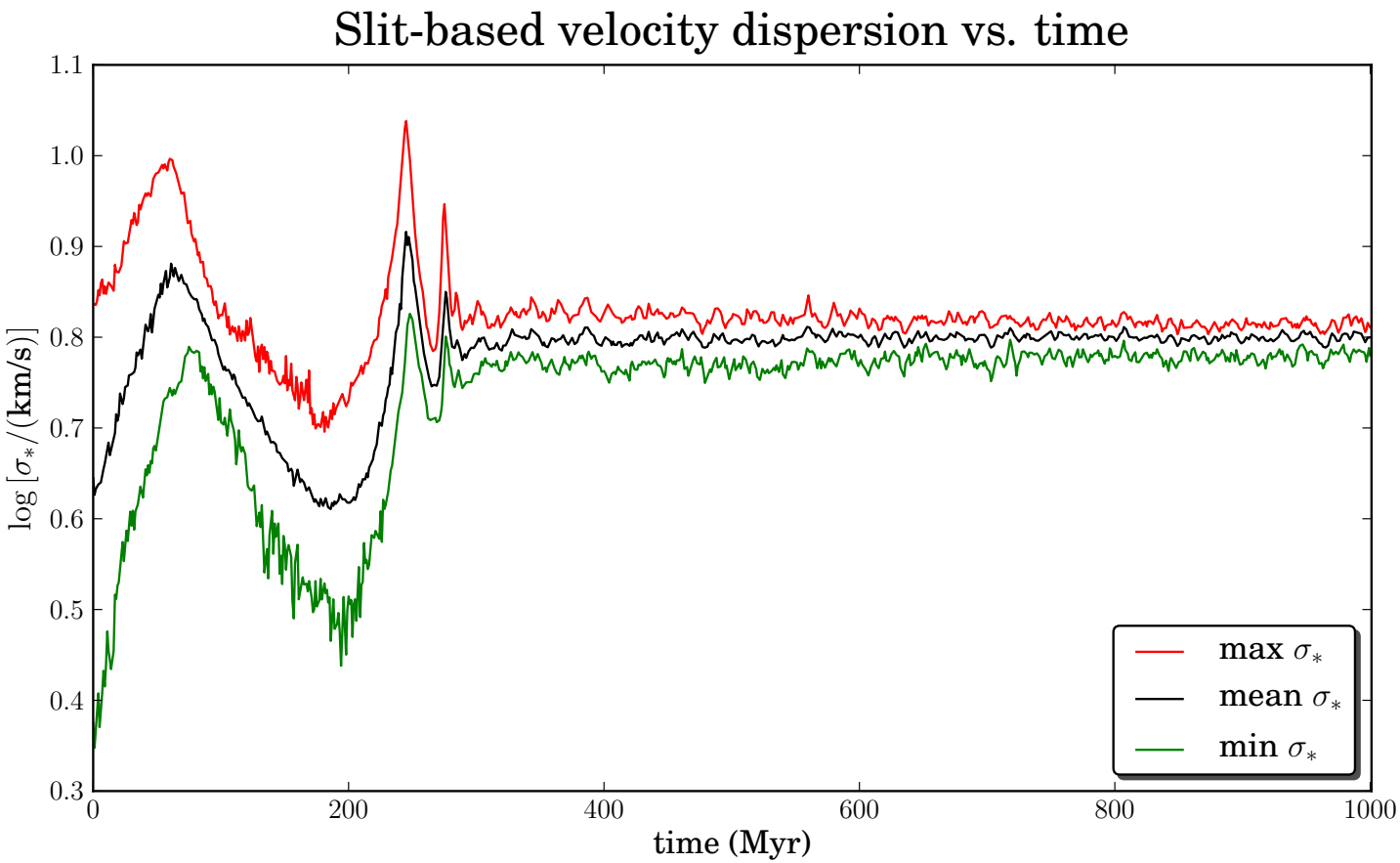

Shear Analysis

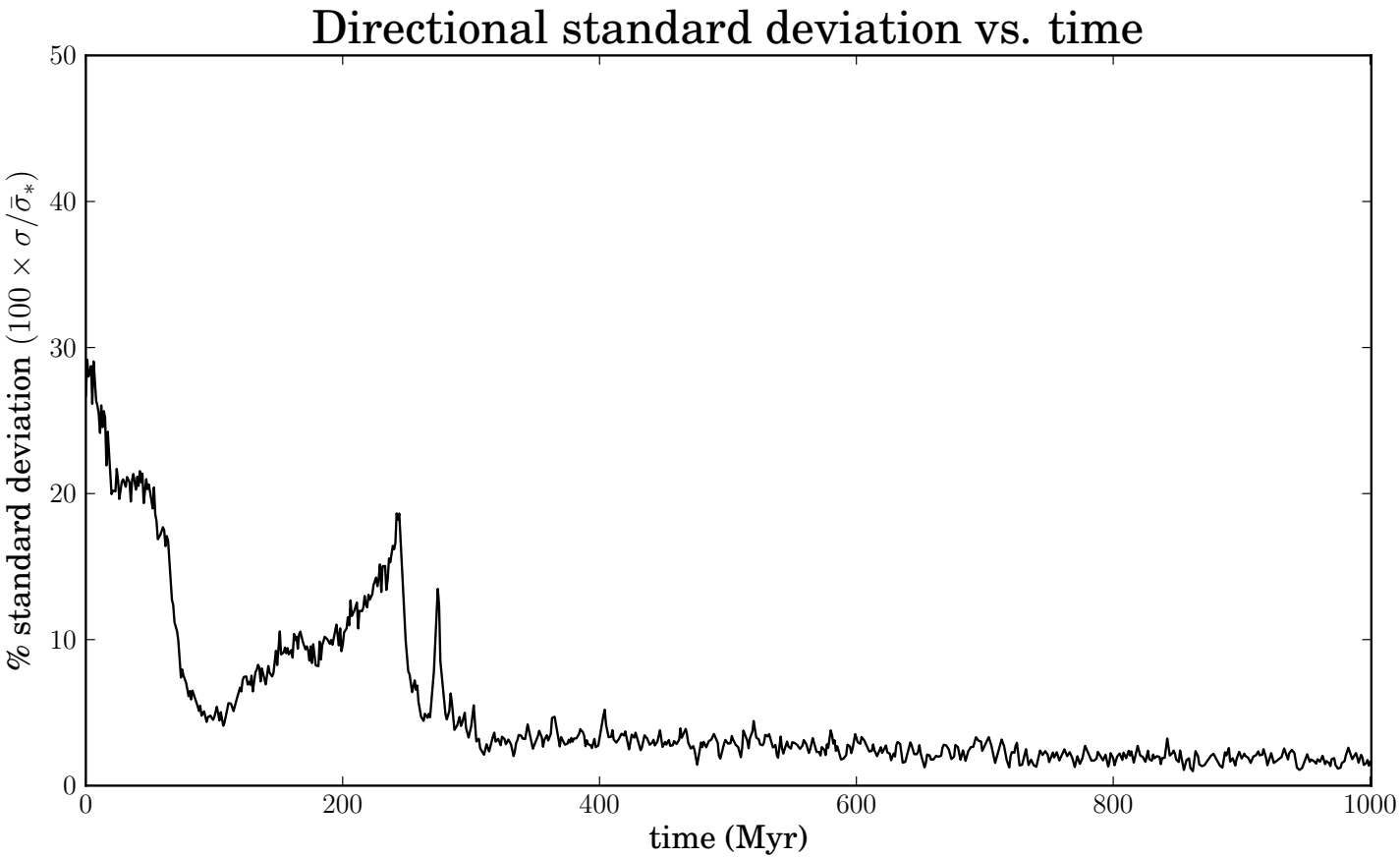

Shear Analysis

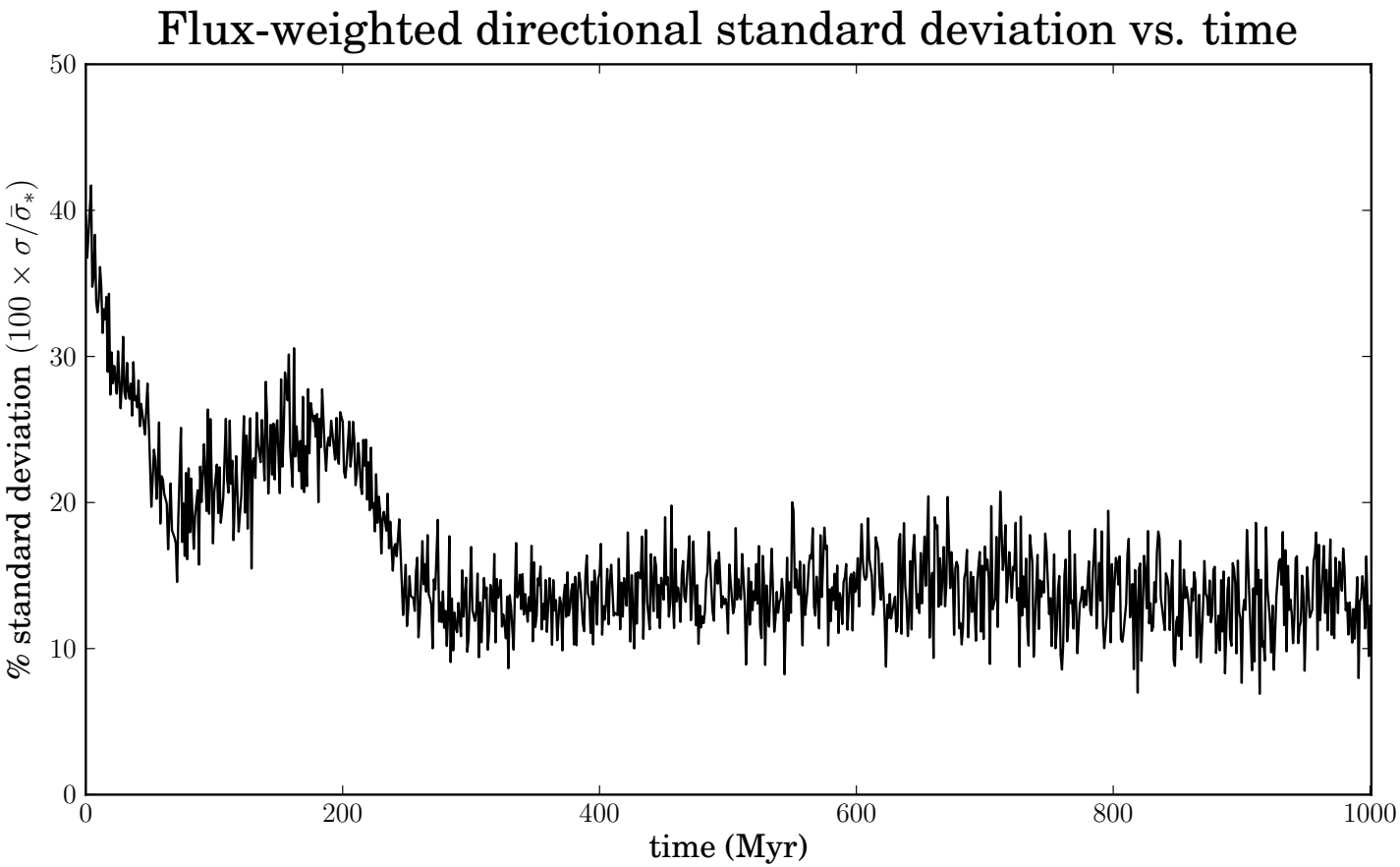

Shear Analysis

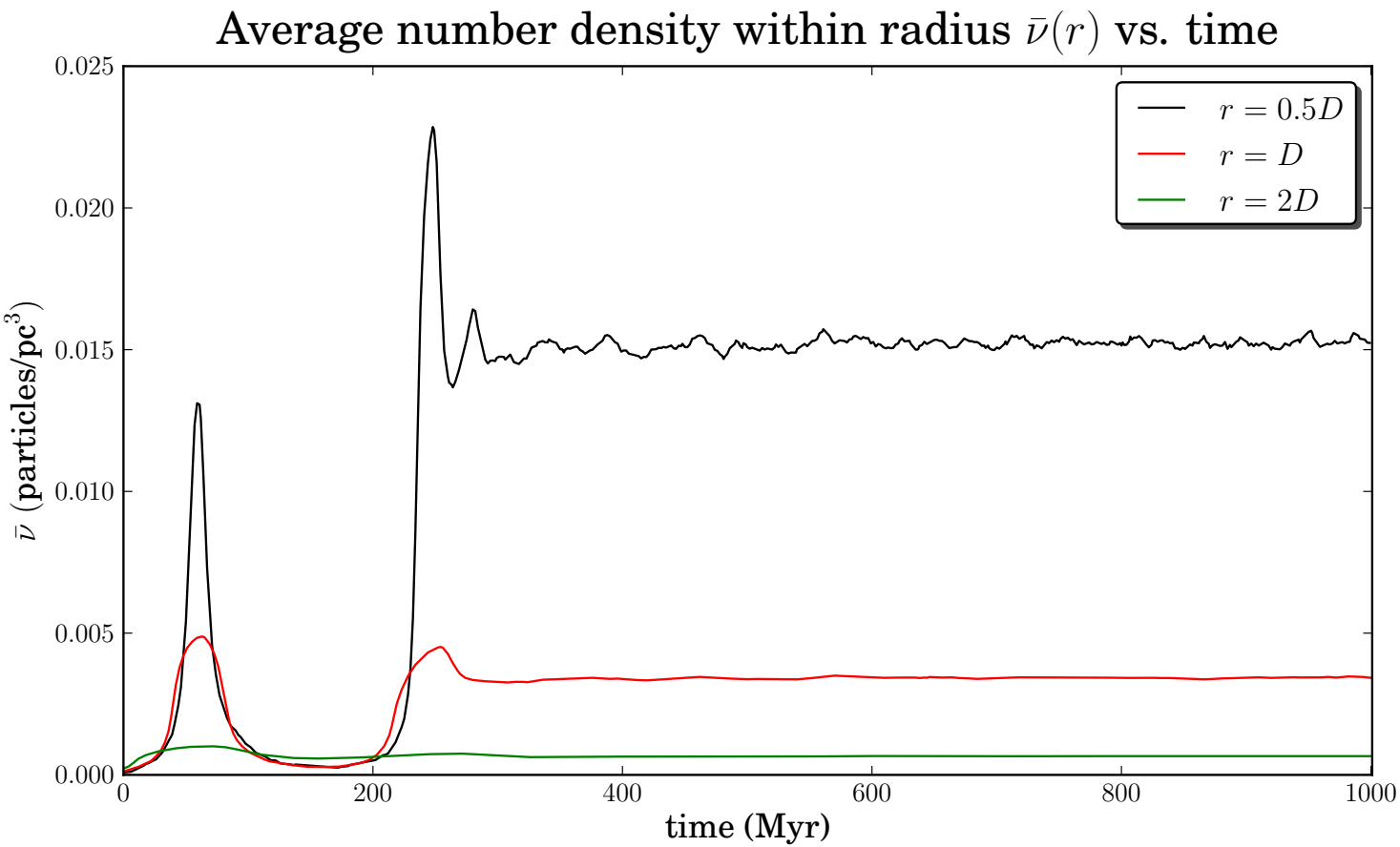

Summary

- More attenuation (larger slab or higher ε) reduces the measured σ_* and increases the scatter $\sigma(\sigma_*)$

Summary

- More attenuation (larger slab or higher ε) reduces the measured σ_* and increases the scatter $\sigma(\sigma_*)$
- Measuring more lines of sight reduces the noise in the measurement of σ_*.

Summary

- More attenuation (larger slab or higher ε) reduces the measured σ_* and increases the scatter $\sigma(\sigma_*)$
- Measuring more lines of sight reduces the noise in the measurement of σ_*.
- σ_* increases sharply during collisions, then undergoes damped oscillations until system reaches equilibrium.

Summary

- More attenuation (larger slab or higher ε) reduces the measured σ_* and increases the scatter $\sigma(\sigma_*)$
- Measuring more lines of sight reduces the noise in the measurement of σ_*.
- σ_* increases sharply during collisions, then undergoes damped oscillations until system reaches equilibrium.
- σ/σ_* increases during collisions, then sharply decreases, and slowly decays long after the collision.

Summary

- More attenuation (larger slab or higher ε) reduces the measured σ_* and increases the scatter $\sigma(\sigma_*)$
- Measuring more lines of sight reduces the noise in the measurement of σ_*.
- σ_* increases sharply during collisions, then undergoes damped oscillations until system reaches equilibrium.
- σ/σ_* increases during collisions, then sharply decreases, and slowly decays long after the collision.
- σ_* increases most dramatically in the direction of the collision.

Summary

- More attenuation (larger slab or higher ε) reduces the measured σ_* and increases the scatter $\sigma(\sigma_*)$
- Measuring more lines of sight reduces the noise in the measurement of σ_*.
- σ_* increases sharply during collisions, then undergoes damped oscillations until system reaches equilibrium.
- σ/σ_* increases during collisions, then sharply decreases, and slowly decays long after the collision.
- σ_* increases most dramatically in the direction of the collision.
- Separating rotation and σ_* isn't straightforward when using aperture-based measurements of σ_*.

Synthesized Spectrum

Combined spectrum (shifted spectra of 9 stellar templates)

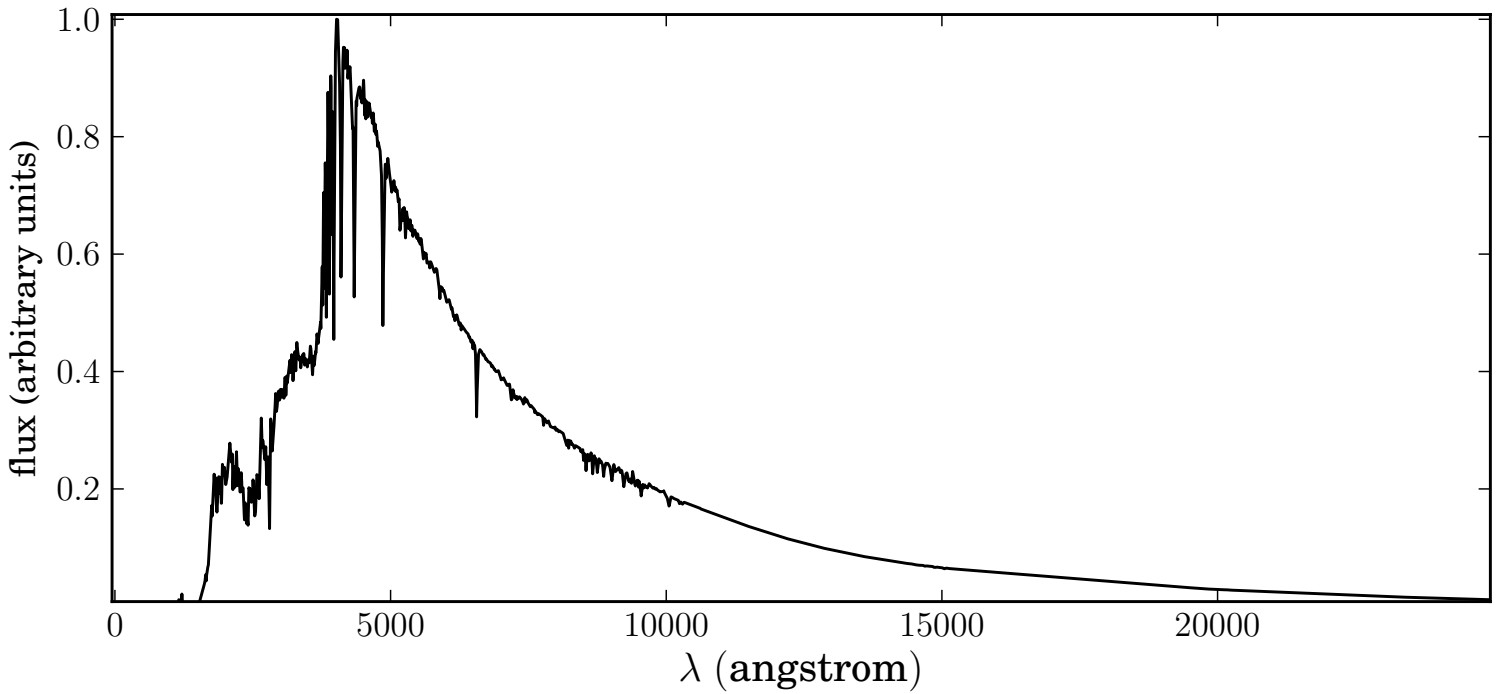

Doppler Broadening Demo

Thin absorption line, $\sigma_* = 2.1$ km/s

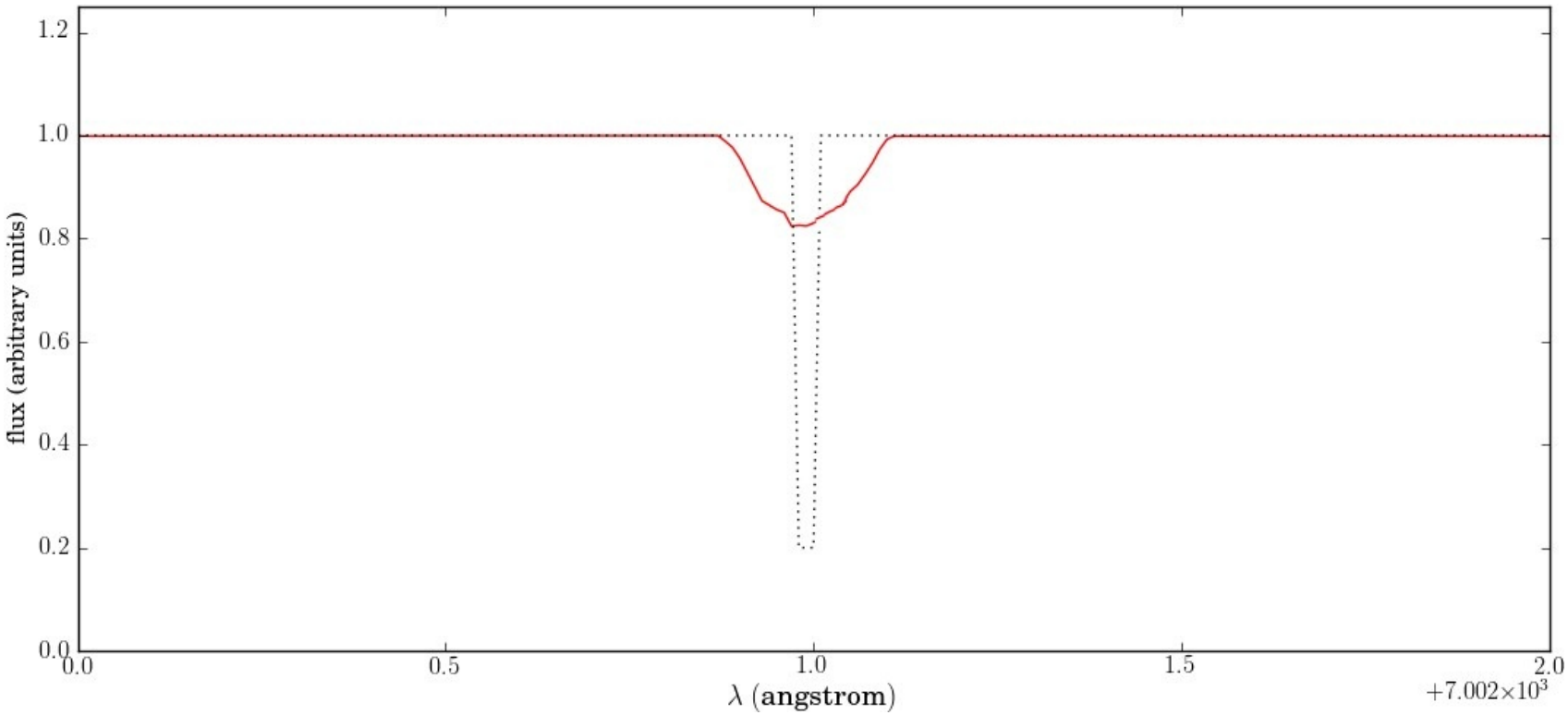

Doppler Broadening Demo

Thin absorption line, $\sigma_* = 5.5$ km/s

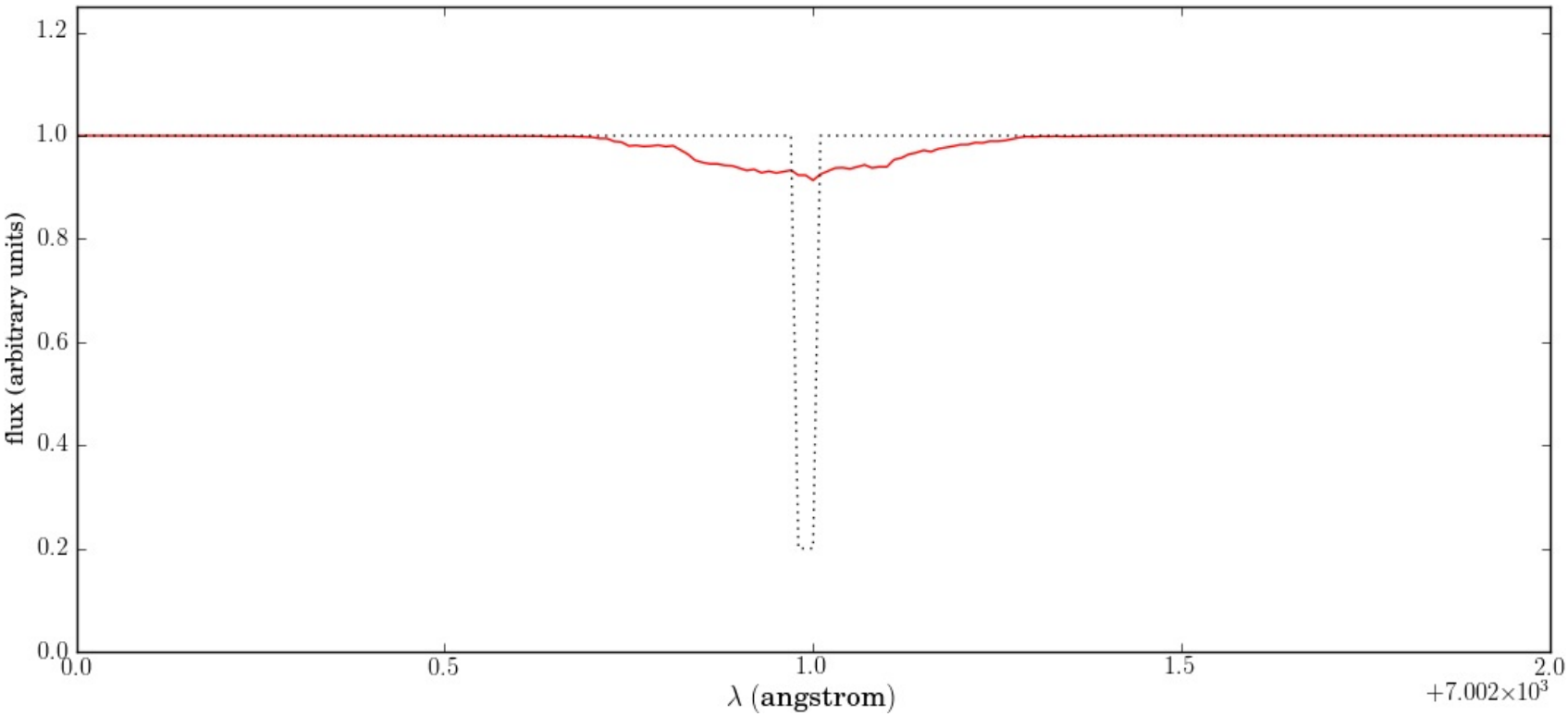

Outline

Thesis Project

The qualifier project did not include:

- dark matter
- super-massive black holes
- gas dynamics
- AGN feedback
- star formation and death
- a realistic treatment of dust extinction
- spheroids of realistic mass and size
- measurements of σ_* consistent with observational technique

Thesis Project

The thesis project will...

- use **GADGET-2** to perform high-resolution dissipational simulations of galaxies including all of the major components missing from the qualifier project.
- use **Sunrise** to realistically treat dust extinction, create galaxy spectra, and perform simulated observations of galaxies.

Thesis Project

The thesis project will...

- use **GADGET-2** to perform high-resolution dissipational simulations of galaxies including all of the major components missing from the qualifier project.
- use **Sunrise** to realistically treat dust extinction, create galaxy spectra, and perform simulated observations of galaxies.
- use observational analysis tools to analyze images and spectra created by Sunrise.

GADGET-2

GADGET-2:

- Highly scalable simulation code written in C, parallelized with MPI.
- Computes gravitational forces using Barnes-Hut tree method (or PM method, if desired).
- Gas / ISM is handled using smoothed-particle hydrodynamics (SPH).
- Gas cooling and heating are included.
- Metallicity of ISM and star particles is tracked.

GADGET-2

- New star particles are created from SPH particles stochastically based on the ISM density and temperature temperature, at a rate motivated by the Kennicutt-Schmidt law.
- ISM metalicity increases in regions surrounding star formation.
- Stars die: SN feedback heats and pressurizes the ISM.
- Accretion onto black hole and resulting feedback can be modeled in several ways. . .

GADGET-2

Method 1: Spherical accretion; thermal feedback

- Accretion occurs at Bondi-Hoyle-Lyttleton rate (limited by $\dot{M}_{Edd}$).
- Some of the accreted mass-energy (10%) is converted to L_{AGN}.
- A small fraction of AGN luminosity (0.5%) couples thermally to ISM.

GADGET-2

Method 1: Spherical accretion; thermal feedback

- Accretion occurs at Bondi-Hoyle-Lyttleton rate (limited by $\dot{M}_{Edd}$).
- Some of the accreted mass-energy (10%) is converted to L_{AGN}.
- A small fraction of AGN luminosity (0.5%) couples thermally to ISM.

Method 2: Non-spherical accretion; momentum feedback

- Accretion occurs as gas (viscously) loses angular momentum (limited by $\dot{M}_{Edd}$).
- A fraction of the accreted mass-energy is converted to L_{AGN}.
- A fraction of the mass-energy couples back to the ISM through momentum transfer.

Sunrise

- A polychromatic, Monte Carlo, radiative transfer code written in C++ and CUDA, parallelized with pthreads.
- Requires shared memory machine with $\gtrsim 32$ GB of RAM.

Sunrise

- A polychromatic, Monte Carlo, radiative transfer code written in C++ and CUDA, parallelized with pthreads.
- Requires shared memory machine with $\gtrsim 32$ GB of RAM.
- Main Input:
  - GADGET-2 Snapshot
  - choice of dust grain model (MW, SMC, LMC, custom)
  - camera information (positions, resolution)

Sunrise

- A polychromatic, Monte Carlo, radiative transfer code written in C++ and CUDA, parallelized with pthreads.
- Requires shared memory machine with $\gtrsim 32$ GB of RAM.
- Main Input:
  - GADGET-2 Snapshot
  - choice of dust grain model (MW, SMC, LMC, custom)
  - camera information (positions, resolution)
- Output: Images and spectra from a collection of virtual cameras.
  - Images of galaxy
  - Doppler shifted spectra of galaxy (each pixel of each image contains a spectrum).

Sunrise

Basic steps:

1. Discretize spatial domain of simulation using adaptive mesh based on distribution of stars and gas.

Sunrise

Basic steps:

1. Discretize spatial domain of simulation using adaptive mesh based on distribution of stars and gas.
2. Assume that the ISM dust content is proportional to the metallicity of ISM.

Sunrise

Basic steps:

1. Discretize spatial domain of simulation using adaptive mesh based on distribution of stars and gas.
2. Assume that the ISM dust content is proportional to the metallicity of ISM.
3. Stellar spectra are based on ages and metallicities (Starburst99 population synthesis model).

Sunrise

Basic steps:

1. Discretize spatial domain of simulation using adaptive mesh based on distribution of stars and gas.
2. Assume that the ISM dust content is proportional to the metallicity of ISM.
3. Stellar spectra are based on ages and metallicities (Starburst99 population synthesis model).
4. Stars younger than 10 Myr are assumed to be star forming region with enhanced dust and PDR; they are modeled using the MappingsIII code (Groves et al., 2008).
5. Shoots $\sim 10^6 - 10^7$ photon bundles from stars through the galaxy.

Collision Analysis

Perform a suite of galaxy collisions using GADGET-2...

- Save GADGET-2 snapshots at ≤ 50 Myr intervals.

Collision Analysis

Perform a suite of galaxy collisions using GADGET-2...

- Save GADGET-2 snapshots at ≤ 50 Myr intervals.
- Analyse velocity dispersion using the standard (mass-weighted) method.

Collision Analysis

Perform a suite of galaxy collisions using GADGET-2...

- Save GADGET-2 snapshots at ≤ 50 Myr intervals.
- Analyse velocity dispersion using the standard (mass-weighted) method.
- For a subset of collisions, run Sunrise to create images and σ_*.

Collision Analysis

Perform a suite of galaxy collisions using GADGET-2...

- Save GADGET-2 snapshots at ≤ 50 Myr intervals.
- Analyse velocity dispersion using the standard (mass-weighted) method.
- For a subset of collisions, run Sunrise to create images and σ_*.
- Compute flux-weighted σ_* from spectra and compare with mass-weighted spectra.

Collision Analysis

Perform a suite of galaxy collisions using GADGET-2. . .

- Save GADGET-2 snapshots at ≤ 50 Myr intervals.
- Analyse velocity dispersion using the standard (mass-weighted) method.
- For a subset of collisions, run Sunrise to create images and σ_*.
- Compute flux-weighted σ_* from spectra and compare with mass-weighted spectra.
- Analyze morphologies (concentration, gini coefficient, asymmetry), colors, and color excesses of systems.

Collision Analysis

Perform a suite of galaxy collisions using GADGET-2. . .

- Save GADGET-2 snapshots at ≤ 50 Myr intervals.
- Analyse velocity dispersion using the standard (mass-weighted) method.
- For a subset of collisions, run Sunrise to create images and σ_*.
- Compute flux-weighted σ_* from spectra and compare with mass-weighted spectra.
- Analyze morphologies (concentration, gini coefficient, asymmetry), colors, and color excesses of systems.
- Look for correlations between morph, color, color excess, and the behavior of σ_* in analogy with Lotz et al.

Trials

- Select configurations for comparison with Johansson et al. and Lotz et al.
- Select broad range of other collisions to mimic the range of collisions observed in nature. Vary:
  - gas fraction
  - mass ratio
  - Hubble type
  - orbital parameters: pro vs. retrograde, apsidal distance, relative velocities
- examine resolution effects (vary N, h, ϵ)
- test the influence of the dust model on measured σ_*.
- evaluate the difference between momentum and thermal AGN feedback.

Further Analysis

Further Analysis:

- Use Cosmological galaxy merger statistics and the results above to predict the fraction of galaxies at a given redshift with relaxed σ_*.
- Predict evolution and scatter of the observed $M_{BH} - \sigma_*$ relation.
- Attempt to create a set of diagnostics based on morphology, colors, and color excesses to determine the state of the measured and "real" σ_* for an observed galaxy.

Research Plan/Schedule

Dec 2010	Build workstation and configure software.
Mar 2011	Finish running low-resolution GADGET-2 test simulations and analyze with Sunrise (for practice). Streamline the spectral and morphological analysis process (Automate as much as possible).
May 2011	Decide on official set of initial configurations and begin running high resolution simulations on supercomputer. Begin Sunrise analysis.
Feb 2012	Finish high-resolution simulations and Sunrise analysis. Begin statistical analysis and writing thesis / publications.
Sept 2012	Finish writing thesis and submitting main results for publication.

References I

Abraham, R. G., van den Bergh, S., & Nair, P. 2003, ApJ, 588, 218

Bennert, V. N., Auger, M. W., Treu, T., Woo, J., & Malkan, M. A. 2010, ArXiv e-prints

DeBuhr, J., Quataert, E., Ma, C., & Hopkins, P. 2009, ArXiv e-prints

Fakhouri, O., Ma, C., & Boylan-Kolchin, M. 2010, MNRAS, 406, 2267

Ferrarese, L., & Merritt, D. 2000, ApJl, 539, L9

Gebhardt, K., et al. 2000, ApJl, 539, L13

Genel, S., Genzel, R., Bouché, N., Naab, T., & Sternberg, A. 2009, ApJ, 701, 2002

Groves, B., Dopita, M. A., Sutherland, R. S., Kewley, L. J., Fischera, J., Leitherer, C., Brandl, B., & van Breugel, W. 2008, The Astrophysical Journal Supplement Series, 176, 438

Hernquist, L. 1990, ApJ, 356, 359

Jogee, S., et al. 2009, ApJ, 697, 1971

Johansson, P. H., Burkert, A., & Naab, T. 2009, ApJl, 707, L184

Jonsson, P. 2006, MNRAS, 372, 2

References II

Jonsson, P., Groves, B. A., & Cox, T. J. 2010, MNRAS, 403, 17

Jonsson, P., & Primack, J. R. 2010, Nature, 15, 509

Lisker, T. 2008, The Astrophysical Journal Supplement Series, 179, 319

Lotz, J. M., Jonsson, P., Cox, T. J., & Primack, J. R. 2008a, MNRAS, 391, 1137

—. 2008b, MNRAS, 391, 1137

—. 2010a, MNRAS, 404, 590

—. 2010b, MNRAS, 404, 575

Maller, A. H., Katz, N., Kereš, D., Davé, R., & Weinberg, D. H. 2006, ApJ, 647, 763

Narayanan, D., et al. 2010, MNRAS, 407, 1701

Shields, G. A., Menezes, K. L., Massart, C. A., & Vanden Bout, P. 2006, ApJ, 641, 683

Springel, V. 2005, MNRAS, 364, 1105

Springel, V., Di Matteo, T., & Hernquist, L. 2005, MNRAS, 361, 776

References III

Tremaine, S., et al. 2002, ApJ, 574, 740

Woo, J., Treu, T., Malkan, M. A., & Blandford, R. D. 2006, ApJ, 645, 900

—. 2008, ApJ, 681, 925

Appendix I: Gravitational Softening

The Motivation: Most of the computational effort in N-body simulations is spent on binary stars.

Solution: Prevent the formation of binary star systems.

- Replace point-particles with extended "fuzzy" particles.
- Particles now represent small *groups* of stars rather than single stars.
- For short distances, replace Newtonian force with another expression corresponding to extended objects.

Appendix I: Gravitational Softening

More Details:

Point particles are "smeared out" into spheres of radius ϵ. The parameter ϵ is known as the softening length.

Examples of Softening Methods:

Plummer Softening

Replace $\frac{Gm_i m_j \mathbf{r}_{ij}}{r_{ij}^3}$ with $\frac{Gm_i m_j \mathbf{r}_{ij}}{\left(r_{ij}^2+\epsilon^2\right)^{3/2}}$

Appendix I: Gravitational Softening

Plummer Softening Spline

$$\mathbf{F}_{ij} = \begin{cases} -\dfrac{Gm_i m_j \mathbf{r}_{ij}}{r_{ij}^3} & \text{for } r > 2\epsilon \\ -\dfrac{Gm_i m_j \mathbf{r}_{ij}}{\left(r_{ij}^2+\epsilon^2\right)^{3/2}} & \text{for } r \leq 2\epsilon \end{cases}$$

- Other methods are also utilized, often incorporating Gaussians and splines.

Appendix II: Leap-Frog Method

Using the centered difference, compute acceleration at time t,

$$\mathbf{a}\left(\mathbf{r}\left(t\right)\right) = \frac{\mathbf{v}\left(t+\delta t\right) - \mathbf{v}\left(t-\delta t\right)}{2\delta t} + \mathcal{O}\left(\delta t^2\right)$$

and the velocity at time $t + \delta t$,

$$\mathbf{v}\left(t+\delta t\right) = \frac{\mathbf{r}\left(t+2\delta t\right) - \mathbf{r}\left(t\right)}{2\delta t} + \mathcal{O}\left(\delta t^2\right)$$

Then rearrange terms so that future values are on the left

$$\mathbf{v}\left(t+\delta t\right) = \mathbf{v}\left(t-\delta t\right) + 2\mathbf{a}\left(\mathbf{r}\left(t\right)\right)\delta t + \mathcal{O}\left(\delta t^3\right)$$

$$\mathbf{r}\left(t+2\delta t\right) = \mathbf{r}\left(t\right) + 2\mathbf{v}\left(t+\delta t\right)\delta t + \mathcal{O}\left(\delta t^3\right)$$

Appendix II: Leap-Frog Method

Using index notation,

$$\mathbf{v}_{i+1} = \mathbf{v}_{i-1} + 2\mathbf{a}_i \delta t + \mathcal{O}\left(\delta t^3\right)$$

$$\mathbf{r}_{i+2} = \mathbf{r}_i + 2\mathbf{v}_{i+1} \delta t + \mathcal{O}\left(\delta t^3\right)$$

This is sometimes written as

$$\mathbf{v}_{i+\frac{1}{2}} = \mathbf{v}_{i-\frac{1}{2}} + \mathbf{a}_i \delta t + \mathcal{O}\left(\delta t^3\right)$$

$$\mathbf{r}_{i+1} = \mathbf{r}_i + \mathbf{v}_{i+\frac{1}{2}} \delta t + \mathcal{O}\left(\delta t^3\right)$$

and other ways...

Appendix II: Leap-Frog Method

drift-kick-drift version:

$$\mathbf{r}_{i+\frac{1}{2}} = \mathbf{r}_i + \mathbf{a}_i \frac{\delta t}{2}$$

$$\mathbf{v}_{i+1} = \mathbf{v}_i + \mathbf{a}_{i+\frac{1}{2}} \delta t$$

$$\mathbf{r}_{i+1} = \mathbf{r}_{i+\frac{1}{2}} + \mathbf{v}_{i+1} \frac{\delta t}{2}$$

where

$$\mathbf{a}_{i+\frac{1}{2}} = \mathbf{a}\left(\mathbf{r}_{i+\frac{1}{2}}\right)$$

kick-drift-kick version:

$$\mathbf{v}_{i+\frac{1}{2}} = \mathbf{v}_i + \mathbf{a}_i \frac{\delta t}{2}$$

$$\mathbf{r}_{i+1} = \mathbf{r}_i + \mathbf{v}_{i+\frac{1}{2}} \frac{\delta t}{2}$$

$$\mathbf{v}_{i+1} = \mathbf{v}_{i+\frac{1}{2}} + \mathbf{a}_{i+1} \frac{\delta t}{2}$$

where

$$\mathbf{a}_{i+1} = \mathbf{a}\left(\mathbf{r}_{i+1}\right)$$

Appendix II: Leap-Frog Method

Comments:

- Even though it is only second order, Leap-Frog yields better results than RK4
- Leap-frog method conserves energy (it is symplectic. . . but only for a fixed step size)
- Kick-drift-kick is the most stable

Appendix III: Smoothed-Particle Hydrodynamics (SPH)

Basic principle:

- Fluid quantities are sampled at discrete points with fixed mass.
- Particles move with the bulk flow of the fluid.
- Particles are *smoothed* over spherical regions of radius h, called "smoothing length".
- Particles are required to overlap.

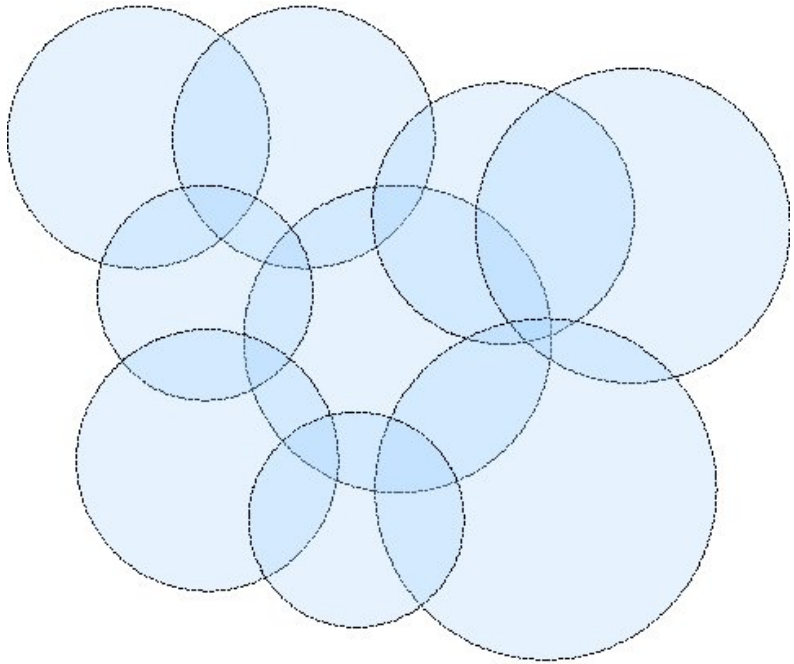

- Specify minimum number of required overlaps, then scale h.

Appendix III: SPH, Basic Formulation

Start with the trivial identity:

$$A(\mathbf{r}) = \int A(\mathbf{r}')\delta\left(\mathbf{r} - \mathbf{r}'\right) d\mathbf{r}'$$

This can be approximated

$$\langle A(\mathbf{r})\rangle \approx \int A(\mathbf{r}')w\left(\mathbf{r} - \mathbf{r}', h\right) d\mathbf{r}'$$

where the smoothing kernel $w(r, h)$ obeys

$$\int w(r, h)dV = 1$$

and

$$\lim_{h\to 0} w(r, h) \longrightarrow \delta(r)$$

Appendix III: SPH, Basic Formulation

$$\langle A(\mathbf{r})\rangle \approx \int A(\mathbf{r}')w\left(\mathbf{r}-\mathbf{r}',h\right)d\mathbf{r}'$$

$$= \int \frac{A(\mathbf{r}')}{\rho\left(\mathbf{r}'\right)}\rho\left(\mathbf{r}'\right)w\left(\mathbf{r}-\mathbf{r}',h\right)d\mathbf{r}'$$

This is approximated as

$$\langle A(\mathbf{r}_i)\rangle \approx \sum_j \left[\rho\left(\mathbf{r}_j\right)V_j\right]\frac{A\left(\mathbf{r}_j\right)}{\rho\left(\mathbf{r}_j\right)}w\left(\mathbf{r}_i-\mathbf{r}_j,h\right)$$

$$= \sum_j m_j\frac{A_j}{\rho_j}w\left(\mathbf{r}_i-\mathbf{r}_j,h\right)$$

Appendix III: SPH, Basic Formulation

We arrive at the approximation

$$\langle A(\mathbf{r}_i)\rangle \approx \sum_j m_j \frac{A_j}{\rho_j} w\left(\mathbf{r}_i - \mathbf{r}_j, h\right)$$

this is analogous to FEM expansion in terms of shape functions.

Example: calculate $\langle \rho(\mathbf{r}_i)\rangle$

$$\langle \rho(\mathbf{r}_i)\rangle \approx \sum_j m_j \frac{\rho_j}{\rho_j} w\left(\mathbf{r}_i - \mathbf{r}_j, h\right) = \sum_j m_j w\left(\mathbf{r}_i - \mathbf{r}_j, h\right)$$

Appendix III: SPH, Basic Formulation

Example: calculate $\langle \mathbf{v}_i \rangle$

$$\langle \mathbf{v}_i \rangle \approx \sum_j \frac{m_j}{\rho_j} \mathbf{v}_j w\left(\mathbf{r}_i - \mathbf{r}_j, h\right)$$

Gradient and divergence are approximated by returning to integral formulation, using integration by parts and vector identities to manipulate the expressions. The results are:

$$\nabla A(\mathbf{r}_i) \approx \langle \nabla A(\mathbf{r}_i) \rangle \approx \sum_j m_j \frac{A_j}{\rho_j} \nabla_i w\left(\mathbf{r}_i - \mathbf{r}_j, h\right)$$

$$\nabla \cdot \mathbf{v}_i \approx \frac{1}{\rho_i} \sum_j \frac{m_j}{\rho_j} \left(\mathbf{v}_i - \mathbf{v}_j\right) \cdot \nabla_i w\left(\mathbf{r}_i - \mathbf{r}_j, h\right)$$

Appendix IV: Bondi-Hoyle-Lyttleton Accretion

The Bondi-Hoyle-Lyttleton Accretion rate:

$$\dot{M} = \frac{4\pi\alpha G^2 M^2 \rho}{(c_s^2 + v_\infty^2)^{3/2}}$$

- α is a resolution mis-match correction term. If the Bondi radius is resolved, $\alpha = 1$
- c_s is the local speed of sound.
- v_∞ is the relative speed of the surrounding gas and the black hole.
- ρ is the density of the local gas.

Appendix V: The Jeans Equation

For completely collisionless, dissipationless systems, the evolution is described by the **collisionless Boltzmann equation**

$$\frac{\partial f}{\partial t} + \mathbf{v} \cdot \nabla f - \nabla \Phi \cdot \frac{\partial f}{\partial \mathbf{v}} = 0$$

Where $f = f(\mathbf{x}, \mathbf{v}, t)$ is the phase space density.

Appendix V: The Jeans Equation

For completely collisionless, dissipationless systems, the evolution is described by the **collisionless Boltzmann equation**

$$\frac{\partial f}{\partial t} + \mathbf{v} \cdot \nabla f - \nabla \Phi \cdot \frac{\partial f}{\partial \mathbf{v}} = 0$$

Where $f = f(\mathbf{x}, \mathbf{v}, t)$ is the phase space density.

In component form,

$$\frac{\partial f}{\partial t} + \sum_{i=1}^{3} \left(v_i \frac{\partial f}{\partial x_i} - \frac{\partial \Phi}{\partial x_i} \frac{\partial f}{\partial v_i} \right) = 0 \qquad (1)$$

Appendix V: The Jeans Equation

$$\frac{\partial f}{\partial t} + \sum_{i=1}^{3} \left(v_i \frac{\partial f}{\partial x_i} - \frac{\partial \Phi}{\partial x_i} \frac{\partial f}{\partial v_i} \right) = 0$$

Integrating over all velocities and using the summation convention,

$$\int \frac{\partial f}{\partial t} d^3\mathbf{v} + \int v_i \frac{\partial f}{\partial x_i} d^3\mathbf{v} - \frac{\partial \Phi}{\partial x_i} \int \frac{\partial f}{\partial v_i} d^3\mathbf{v} = 0$$

Appendix V: The Jeans Equation

$$\frac{\partial f}{\partial t} + \sum_{i=1}^{3} \left(v_i \frac{\partial f}{\partial x_i} - \frac{\partial \Phi}{\partial x_i} \frac{\partial f}{\partial v_i} \right) = 0$$

Integrating over all velocities and using the summation convention,

$$\int \frac{\partial f}{\partial t} d^3\mathbf{v} + \int v_i \frac{\partial f}{\partial x_i} d^3\mathbf{v} - \frac{\partial \Phi}{\partial x_i} \int \frac{\partial f}{\partial v_i} d^3\mathbf{v} = 0$$

Note that v_i does not depend on x_i and the integration domain (all velocities) is independent of t. Then...

Appendix V: The Jeans Equation

$$\frac{\partial f}{\partial t} + \sum_{i=1}^{3} \left(v_i \frac{\partial f}{\partial x_i} - \frac{\partial \Phi}{\partial x_i} \frac{\partial f}{\partial v_i} \right) = 0$$

Integrating over all velocities and using the summation convention,

$$\int \frac{\partial f}{\partial t} d^3\mathbf{v} + \int v_i \frac{\partial f}{\partial x_i} d^3\mathbf{v} - \frac{\partial \Phi}{\partial x_i} \int \frac{\partial f}{\partial v_i} d^3\mathbf{v} = 0$$

Note that v_i does not depend on x_i and the integration domain (all velocities) is independent of t. Then...

$$\frac{\partial}{\partial t} \int f d^3\mathbf{v} + \frac{\partial}{\partial x_i} \int v_i f d^3\mathbf{v} - \frac{\partial \Phi}{\partial x_i} \int \frac{\partial f}{\partial v_i} d^3\mathbf{v} = 0$$

Appendix V: The Jeans Equation

$$\frac{\partial}{\partial t}\int f d^3\mathbf{v} + \frac{\partial}{\partial x_i}\int v_i f d^3\mathbf{v} - \frac{\partial \Phi}{\partial x_i}\int \frac{\partial f}{\partial v_i} d^3\mathbf{v} = 0$$

The red term vanishes upon using the divergence theorem and noting that stars have zero probability of having infinite speed.

Appendix V: The Jeans Equation

$$\frac{\partial}{\partial t}\int f d^3\mathbf{v} + \frac{\partial}{\partial x_i}\int v_i f d^3\mathbf{v} - \frac{\partial \Phi}{\partial x_i}\int \frac{\partial f}{\partial v_i} d^3\mathbf{v} = 0$$

The red term vanishes upon using the divergence theorem and noting that stars have zero probability of having infinite speed.

Thus

$$\frac{\partial}{\partial t}\int f d^3\mathbf{v} + \frac{\partial}{\partial x_i}\int v_i f d^3\mathbf{v} = 0$$

Appendix V: The Jeans Equation

$$\frac{\partial}{\partial t}\int f d^3\mathbf{v} + \frac{\partial}{\partial x_i}\int v_i f d^3\mathbf{v} = 0$$

Defining the stellar number density $\nu(\mathbf{x})$ and the mean stellar velocity $\bar{\mathbf{v}}(\mathbf{x})$:

$$\nu \equiv \int f d^3\mathbf{v} \qquad \text{and} \qquad \bar{v}_i \equiv \frac{1}{\nu}\int f v_i \, d^3\mathbf{v}$$

Appendix V: The Jeans Equation

$$\frac{\partial}{\partial t}\int f d^3\mathbf{v} + \frac{\partial}{\partial x_i}\int v_i f d^3\mathbf{v} = 0$$

Defining the stellar number density $\nu(\mathbf{x})$ and the mean stellar velocity $\bar{\mathbf{v}}(\mathbf{x})$:

$$\nu \equiv \int f d^3\mathbf{v} \qquad \text{and} \qquad \bar{v}_i \equiv \frac{1}{\nu}\int f v_i \, d^3\mathbf{v}$$

The equation becomes

$$\frac{\partial \nu}{\partial t} + \frac{\partial(\nu \bar{v}_i)}{\partial x_i} = 0 \tag{2}$$

This is a statement of the conservation of particle number.

Appendix V: The Jeans Equation

Multiplying the collisionless Boltzmann equation (1) by v_i and repeating the process of integrating over all velocities, yields

$$\frac{\partial(\nu\bar{v}_j)}{\partial t} + \frac{\partial(\nu\overline{v_i\,v_j})}{\partial x_i} + \frac{\partial\Phi}{\partial x_i}\nu\delta_{ij} = 0$$

where

$$\overline{v_i\,v_j} \equiv \frac{1}{\nu}\int v_i\,v_j f d^3\mathbf{v}.$$

Appendix V: The Jeans Equation

Multiplying the collisionless Boltzmann equation (1) by v_i and repeating the process of integrating over all velocities, yields

$$\frac{\partial(\nu\bar{v}_j)}{\partial t} + \frac{\partial(\nu\overline{v_i\,v_j})}{\partial x_i} + \frac{\partial\Phi}{\partial x_i}\nu\delta_{ij} = 0$$

where

$$\overline{v_i\,v_j} \equiv \frac{1}{\nu}\int v_i\,v_j f d^3\mathbf{v}.$$

Simplifying,

$$\frac{\partial(\nu\bar{v}_j)}{\partial t} + \frac{\partial(\nu\overline{v_i\,v_j})}{\partial x_i} + \nu\frac{\partial\Phi}{\partial x_j} = 0 \qquad (3)$$

Appendix V: The Jeans Equation

In summary:

$$\frac{\partial \nu}{\partial t} + \frac{\partial(\nu \bar{v}_i)}{\partial x_i} = 0 \tag{2}$$

$$\frac{\partial(\nu \bar{v}_j)}{\partial t} + \frac{\partial(\nu \overline{v_i v_j})}{\partial x_i} + \nu \frac{\partial \Phi}{\partial x_j} = 0 \tag{3}$$

Appendix V: The Jeans Equation

In summary:

$$\frac{\partial \nu}{\partial t} + \frac{\partial(\nu \bar{v}_i)}{\partial x_i} = 0 \quad (2)$$

$$\frac{\partial(\nu \bar{v}_j)}{\partial t} + \frac{\partial(\nu \overline{v_i v_j})}{\partial x_i} + \nu \frac{\partial \Phi}{\partial x_j} = 0 \quad (3)$$

Multiplying eq.(2) by $\bar{v}_j$, subtracting this from eq.(3), and simplifying

Appendix V: The Jeans Equation

In summary:

$$\frac{\partial \nu}{\partial t} + \frac{\partial(\nu \bar{v}_i)}{\partial x_i} = 0 \quad (2)$$

$$\frac{\partial(\nu \bar{v}_j)}{\partial t} + \frac{\partial(\nu \overline{v_i v_j})}{\partial x_i} + \nu \frac{\partial \Phi}{\partial x_j} = 0 \quad (3)$$

Multiplying eq.(2) by $\bar{v}_j$, subtracting this from eq.(3), and simplifying

$$\nu \frac{\partial \bar{v}_j}{\partial t} + \frac{\partial(\nu \overline{v_i v_j})}{\partial x_i} + \nu \frac{\partial \Phi}{\partial x_j} - \bar{v}_j \frac{\partial(\nu \bar{v}_i)}{\partial x_i} = 0 \quad (4)$$

Appendix V: The Jeans Equation

$$\nu \frac{\partial \bar{v}_j}{\partial t} + \frac{\partial (\nu \overline{v_i v_j})}{\partial x_i} + \nu \frac{\partial \Phi}{\partial x_j} - \bar{v}_j \frac{\partial (\nu \bar{v}_i)}{\partial x_i} = 0$$

The term $\overline{v_i v_j}$ can be written as the sum of streaming and random parts:

$$\overline{v_i v_j} = \bar{v}_i \bar{v}_j + \sigma_{ij}^2 \tag{5}$$

where

$$\sigma_{ij}^2 \equiv \overline{(v_i - \bar{v}_i)(v_j - \bar{v}_j)}$$

σ_{ij}^2 is the covariance of (v_i, v_j), AKA the velocity dispersion tensor.

Appendix V: The Jeans Equation

$$\nu\frac{\partial\bar{v}_j}{\partial t}+\frac{\partial(\nu\overline{v_i\,v_j})}{\partial x_i}+\nu\frac{\partial\Phi}{\partial x_j}-\bar{v}_j\frac{\partial(\nu\bar{v}_i)}{\partial x_i}=0$$

The term $\overline{v_i\,v_j}$ can be written as the sum of streaming and random parts:

$$\overline{v_i\,v_j}=\bar{v}_i\,\bar{v}_j+\sigma_{ij}^2 \tag{5}$$

where

$$\sigma_{ij}^2\equiv\overline{(v_i-\bar{v}_i)(v_j-\bar{v}_j)}$$

σ_{ij}^2 is the covariance of (v_i,v_j), AKA the velocity dispersion tensor.

Now we substitute Eq.(5) into our equation...

Appendix V: The Jeans Equation

$$\nu \frac{\partial \bar{v}_j}{\partial t} + \frac{\partial(\nu \bar{v}_i \bar{v}_j)}{\partial x_i} + \frac{\partial(\nu \sigma_{ij}^2)}{\partial x_i} + \nu \frac{\partial \Phi}{\partial x_j} - \bar{v}_j \frac{\partial(\nu \bar{v}_i)}{\partial x_i} = 0$$

Appendix V: The Jeans Equation

$$\nu\frac{\partial\bar{v}_j}{\partial t}+\frac{\partial(\nu\bar{v}_i\bar{v}_j)}{\partial x_i}+\frac{\partial(\nu\sigma_{ij}^2)}{\partial x_i}+\nu\frac{\partial\Phi}{\partial x_j}-\bar{v}_j\frac{\partial(\nu\bar{v}_i)}{\partial x_i}=0$$

Simplifying,

$$\nu\frac{\partial\bar{v}_j}{\partial t}+\nu\bar{v}_i\frac{\partial\bar{v}_j}{\partial x_i}+\frac{\partial(\nu\sigma_{ij}^2)}{\partial x_i}+\nu\frac{\partial\Phi}{\partial x_j}=0$$

Appendix V: The Jeans Equation

$$\nu\frac{\partial\bar{v}_j}{\partial t}+\frac{\partial(\nu\bar{v}_i\bar{v}_j)}{\partial x_i}+\frac{\partial(\nu\sigma_{ij}^2)}{\partial x_i}+\nu\frac{\partial\Phi}{\partial x_j}-\bar{v}_j\frac{\partial(\nu\bar{v}_i)}{\partial x_i}=0$$

Simplifying,

$$\nu\frac{\partial\bar{v}_j}{\partial t}+\nu\bar{v}_i\frac{\partial\bar{v}_j}{\partial x_i}+\frac{\partial(\nu\sigma_{ij}^2)}{\partial x_i}+\nu\frac{\partial\Phi}{\partial x_j}=0$$

Upon rearranging, this becomes

$$\nu\frac{\partial\bar{v}_j}{\partial t}+\nu\bar{v}_i\frac{\partial\bar{v}_j}{\partial x_i}=-\nu\frac{\partial\Phi}{\partial x_j}-\frac{\partial(\nu\sigma_{ij}^2)}{\partial x_i} \tag{6}$$

This is known as the **Jeans equation**.